Article:
FEWSTER, CHRISTOPHER and KIRK-KARAKAYA, HARKAN (2025) Repeated quantum backflow and overflow. Proceedings of the Royal Society A: Mathematical, Physical and Engineering Sciences. 20250577. ISSN: 0080-4630

https://doi.org/10.1098/rspa.2025.0577

PROCEEDINGS A

royalsocietypublishing.org/journal/rspa

Research

Cite this article: Fewster CJ, Kirk-Karakaya HJ. 2025 Repeated quantum backflow and overflow. *Proc. R. Soc. A* **481**: 20250577. https://doi.org/10.1098/rspa.2025.0577

Received: 3 July 2025
Accepted: 28 October 2025

Subject Areas:
mathematical physics, quantum physics

Keywords:
quantum backflow, quantum advantage, numerical acceleration

Author for correspondence:
Christopher J. Fewster
e-mail: chris.fewster@york.ac.uk

Electronic supplementary material is available online at https://doi.org/10.6084/m9.figshare.c.8174360.

THE ROYAL SOCIETY PUBLISHING

Repeated quantum backflow and overflow

Christopher J. Fewster[1,2] and Harkan J. Kirk-Karakaya[1]

[1]Department of Mathematics, and [2]York Centre for Quantum Technologies,University of York, Heslington, York YO10 5DD, UK

CJF, 0000-0001-8915-5321; KJK-K, 0009-0007-8335-0004

Quantum particles moving in one dimension with rightwards momentum can exhibit the surprising phenomenon of quantum backflow (QB): a net probability transfer to the left-hand half-line over a finite time interval. We generalize this phenomenon by considering the sum of probability differences for M disjoint time intervals. In classical mechanics, the total backflow lies in the interval $[-1, 0]$ for all M, indicating rightwards probability transfer. By contrast, we show that the maximum M-fold QB is positive and unbounded from above as M increases, demonstrating the existence of repeated backflow. For $M \geq 2$, a new phenomenon of 'quantum overflow' is discovered: there are states whose total backflow is below -1, which is impossible for classical particles. The extent of the backflow and overflow effects is described by a hierarchy of backflow and overflow functions and constants, of which the $M = 1$ backflow constant was first studied by Bracken and Melloy. Limiting cases of the backflow and overflow functions are studied, including cases in which two disjoint intervals merge. The analytical results are supported by detailed numerical investigations. Using numerical acceleration methods, we obtain a new estimate of the Bracken–Melloy constant of 0.0384506, slightly lower than the previously accepted value of 0.038452.

1. Introduction

Quantum backflow (QB) is a counterintuitive phenomenon in which a free quantum mechanical particle on the line, in a state with purely rightwards momentum, can exhibit a temporary probability transfer to the left-hand half-line. Here, we understand 'purely rightwards

momentum' or 'purely positive-momentum' to mean that the measured value of the momentum would be non-negative with probability 1, or equivalently that the support of the wavefunction in momentum space is contained in the positive half-line. The existence of states exhibiting backflow has been known since at least 1969, when Allcock [1] showed that there exist states with purely positive momentum whose quantum mechanical current at the origin can be arbitrarily negative.

The first detailed study of QB was conducted in 1994 by Bracken & Melloy [2]. They showed that for states that exhibit QB the probability backflow is bounded by a state independent dimensionless value $0 < c_{\mathrm{BM}} < 1$, independent of $\hbar$, which they calculated to be $c_{\mathrm{BM}} \approx 0.04$ [2], by showing that c_{BM} is the largest value in the spectrum of a bounded self-adjoint operator. There have since been two further calculations of c_{BM} to date, first by Eveson *et al.* ($c_{\mathrm{BM}} \approx 0.03845(2)$) [3] and shortly thereafter by Penz *et al.* ($c_{\mathrm{BM}} \approx 0.0384517$) [4]. The first non-trivial upper bound on the backflow constant was calculated only recently by Trillo *et al.* to be $c_{\mathrm{BM}} < 0.072$ [5]. Owing to the small value of c_{BM}, experimental verification of QB is an ongoing effort. Goussev has shown that when considering an angular analogue of QB for a particle on a ring, the associated maximum possible backflow is larger than in the linear case with $c_{\mathrm{ring}} \approx 2.6\, c_{\mathrm{BM}}$ [6]. Angular QB has also been studied in the case of a charged massless fermion [7]. Palmero *et al.* [8] have shown how QB could be experimentally verified by measuring density fluctuations in a Bose–Einstein condensate. Bracken has explored a whole family of QB related problems where the quantum states considered have their momentum restricted to $p > p_0$ for some fixed p_0 not necessarily positive [9]. Other variations of QB that have been considered include but are not limited to: QB in two dimensions [10], QB in a relativistic setting [11], the relation between QB and the local wave number [12] and QB across a black hole horizon [13]. Finally, Bostelmann *et al.* [14] studied the extent to which scattering states exhibit the backflow effect for general short-range potentials, while Yearsley & Halliwell showed that the dependency of the maximal QB on $\hbar$ reappears [15] once a realistic measurement apparatus is considered.

Previously, QB has only ever been considered over a single fixed time interval $[t_1, t_2]$. As first shown by Bracken & Melloy, the associated spectrum of backflow values is independent of t_1 and t_2 [2]. In this paper (following a suggestion by Reinhard Werner) we consider the question of quantum backflow over multiple disjoint time intervals. Given an integer $M \geq 1$ and a strictly increasing list of times $\langle \boldsymbol{t}_M \rangle = \langle t_1, \ldots, t_{2M} \rangle$, we study the total backflow,

$$\Delta^{(M)}_{\langle \boldsymbol{t}_M \rangle}(\psi) = \sum_{j=1}^{M} (\mathrm{Prob}_\psi(X < 0 | t = t_{2j}) - \mathrm{Prob}_\psi(X < 0 | t = t_{2j-1})), \tag{1.1}$$

exhibited by quantum state ψ over the union of the time intervals $[t_1, t_2], \ldots, [t_{2M-1}, t_{2M}]$. A basic question is whether or not the total backflow is also limited by the Bracken–Melloy constant, or whether increasing M can increase the amount of backflow beyond c_{BM}. In other words, are there states which exhibit repeated periods of significant backflow? Further, as a sum of M probability differences, $\Delta^{(M)}_{\langle \boldsymbol{t}_M \rangle}(\psi)$ is, *a priori*, bounded between $\pm M$. Can the maximum total backflow grow unboundedly as $M \to \infty$? Are there states in which one finds $\Delta^{(M)}_{\langle \boldsymbol{t}_M \rangle}(\psi) < -1$, i.e. in which more than unit probability is transferred to the right-hand half-line, in total, over the given intervals? If so, is this effect unbounded as $M \to \infty$? Are the answers to the previous questions different for classical particle mechanics?

We shall answer all these question affirmatively. For M time intervals of equal duration, separated by gaps of the same duration, we show that there are positive-momentum states ψ_M so that $\Delta^{(M)}_{\langle \boldsymbol{t}_M \rangle}(\psi_M) \to \infty$, at least as fast as $\mathcal{O}(M^{1/4})$. Moreover, we discover the new phenomenon that, for $M \geq 2$, there are indeed states with $\Delta^{(M)}_{\langle \boldsymbol{t}_M \rangle}(\psi) < -1$, an effect that we call *quantum overflow*. For the intervals of equal duration separated by gaps of the same duration, we shall prove that there are positive-momentum states φ_M with $\Delta^{(M)}_{\langle \boldsymbol{t}_M \rangle}(\varphi_M) \to -\infty$, at least as fast as $\mathcal{O}(M^{1/4})$. Thus, both QB and overflow are unbounded in the limit of large M. By contrast, the total backflow of a classical particle is constrained to $[-1, 0]$, independent of M. Our analytical results are complemented by a numerical investigation of the magnitude of the backflow and overflow

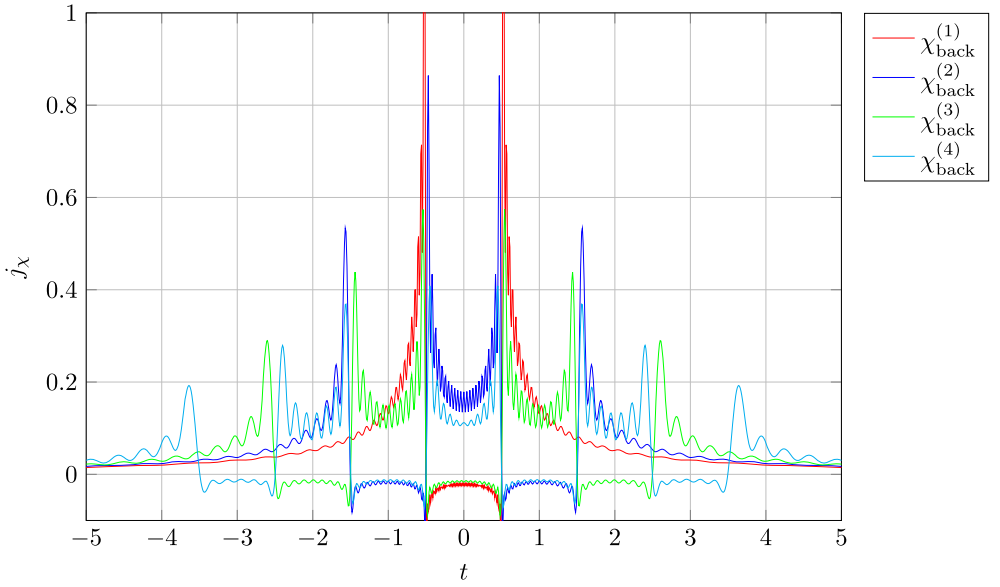

Figure 1. Probability flux at $x = 0$ of the M-fold backflow states $\chi^{(M)}_{\text{back}}$ computed in §5b.

effects for $M \leq 4$. As has been pointed out by one of the referees, overflow could be studied profitably without the restriction to positive momentum. Here, we keep the restriction because it turns out that there is some interplay between the backflow and overflow phenomena in the positive-momentum case. The exploration of overflow in greater generality is left for future work.

Before continuing, we give a preview of some numerical results that are discussed in greater depth below. In §5b, we describe how sequences of states may be found that display significant backflow or overflow for a given set of intervals. Consider in particular M equally spaced intervals of an equal duration that will be chosen as the unit of time in the following discussion. Fixing the unit of mass to be twice the mass of the quantum particle, the unit of length is then fixed so that $\hbar = 1$. The states $\chi^{(M)}_{\text{back}}$ are drawn from calculations reported in §5b and exhibit M-fold backflow over the M time intervals $[-M + 2k + 1/2, -M + 2k + 3/2]$ for $0 \leq k \leq M - 1$, with total backflow 0.0350766, 0.0543496, 0.0684048 and 0.0797003 for $M = 1, 2, 3, 4$, respectively. Figure 1 plots the probability flux at $x = 0$ against time, and shows that the flux is negative in the stated time intervals. The position probability density plots for these states (figures 15 and 16 in §5b) display $M + 1$ main peaks (some with substructure), symmetrically distributed about $x = 0$.

The time evolution of the position probability density in the $M = 2$ case is illustrated in figure 2 for times $-1.5 \leq t \leq 1.5$. In broad outline, the three main peaks move to the right, while nonetheless reshaping so that probability flows to the left-hand half-line during the time intervals $[-1.5, -0.5]$ and $[0.5, 1.5]$. At $t = -1.5$ the leading peak lies in $x > 0$ and is higher than the other two; by $t = -0.5$, the leading peak has diminished while the central peak and the trailing peak, still in $x < 0$, have grown. By $t = 0.5$, the central peak is dominant, lying in $x > 0$, and over the time interval $[0.5, 1.5]$ this peak diminishes while the trailing peak, still in $x < 0$, grows. These reshapings are the result of constructive and destructive interference between the slow-moving main peaks and higher-frequency pulses that move through at a higher velocity. As it evolves, the wavepacket spreads on a characteristic time scale $t_S = m(\Delta X)/\Delta P$, where ΔX and ΔP are the dispersions of position and momentum at $t = 0$. For $\chi^{(2)}_{\text{back}}$, we computed $t_S \sim 1.7$, showing that backflow takes place on comparable time scales to t_S, and indeed figure 1 shows that the probability flux is positive for times $|t| \gtrsim t_S$.

The calculations in §5b also provide states $\chi^{(M)}_{\text{over}}$ exhibiting significant overflow on the M equally spaced intervals of equal (unit) duration given above, with total backflow equal to -1.00213, -1.00628 and -1.01122 for $M = 2, 3, 4$, respectively. Figure 3 shows the time evolution of

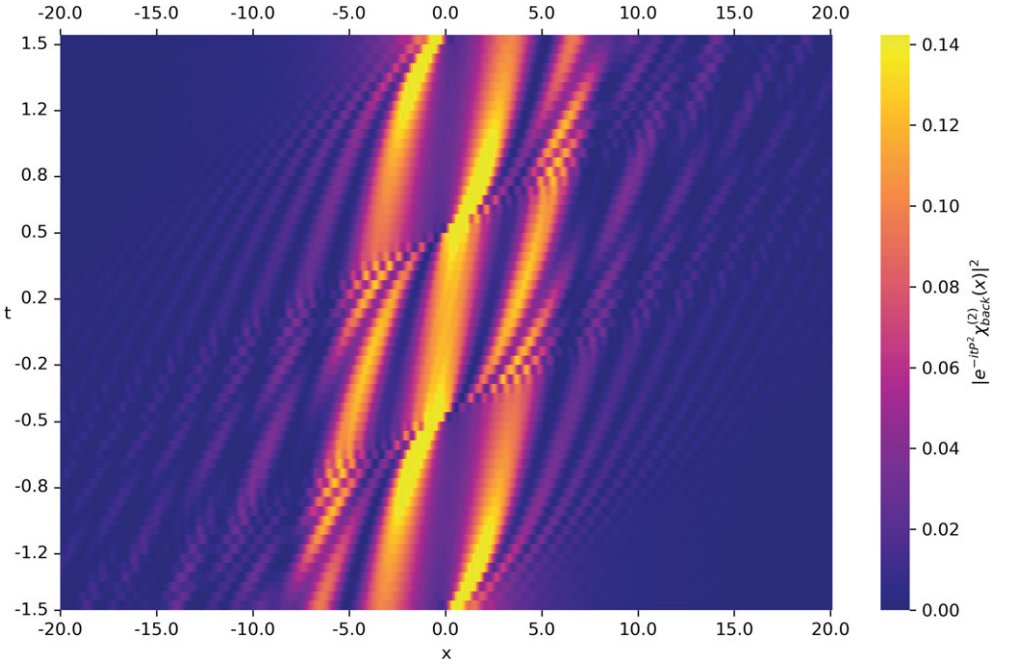

Figure 2. Time evolution of the position probability density for the $M = 2$ backflow state $\chi^{(2)}_{\text{back}}$.

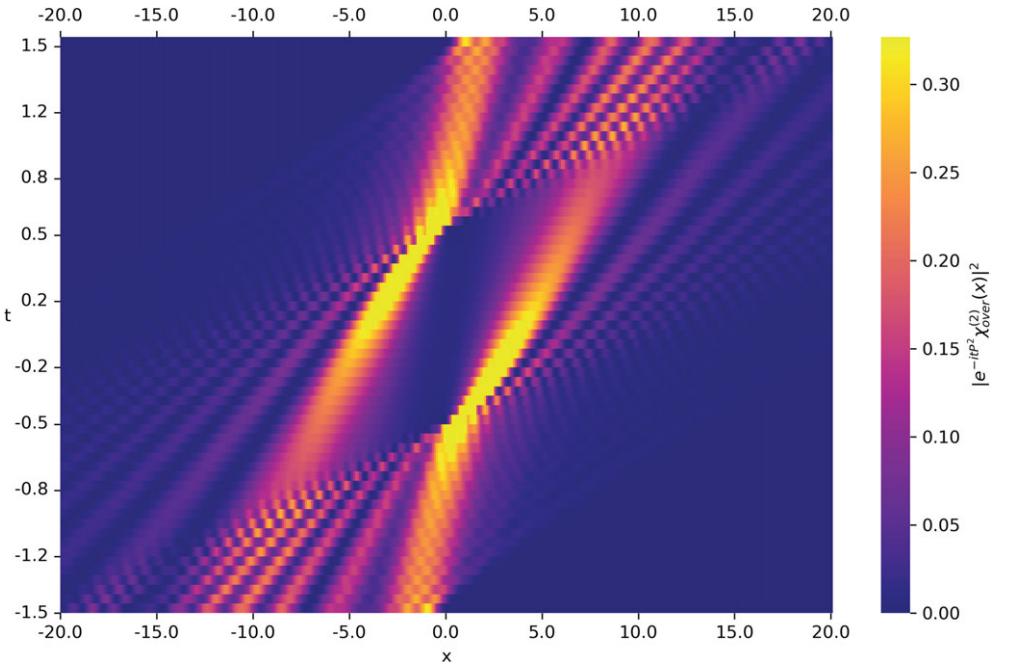

Figure 3. Time evolution of the position probability density for the $M = 2$ overflow state $\chi^{(2)}_{\text{over}}$.

the position probability density evolution for $\chi^{(2)}_{\text{over}}$, which has spreading time $t_S \sim 1.4$. At $t = -1.5$ the bulk of the probability distribution lies in $x < 0$. During the initial time period $[-1.5, -0.5]$ the slow-moving main peak and faster high-frequency peaks move forwards and net probability flows into $x > 0$. At $t = -0.5$ the distribution has two main peaks with the dominant one in $x > 0$; during the time interval $[-0.5, 0.5]$, these peaks reshape and probability flows backwards into

the negative half-line, before again flowing forwards in the final period [0.5, 1.5]. Plots of the flux (given in the electronic supplementary material, §J) show that the overflow states for $M = 2, 3, 4$ all exhibit backflow between the overflow intervals. This is in line with the following elementary argument. Note that

$$\Delta^{(2)}_{\langle t_1,t_2,t_3,t_4\rangle}(\psi) = \Delta^{(1)}_{\langle t_1,t_4\rangle}(\psi) - \Delta^{(1)}_{\langle t_2,t_3\rangle}(\psi) \geq -1 - \Delta^{(1)}_{\langle t_2,t_3\rangle}(\psi), \tag{1.2}$$

because overflow does not occur for $M = 1$. Thus, if ψ exhibits 2-fold overflow for intervals $[t_1, t_2]$ and $[t_3, t_4]$, then $\Delta^{(2)}_{\langle t_1,t_2,t_3,t_4\rangle}(\psi) < -1$ and consequently $\Delta^{(1)}_{\langle t_2,t_3\rangle}(\psi) > 0$, which shows that ψ also exhibits backflow over $[t_2, t_3]$.

To gain some understanding into why M-fold backflow can exceed the Bracken–Melloy limit, consider a normalized positive-momentum state ψ that exhibits backflow $\Delta = \Delta^{(1)}_{\langle t_1,t_2\rangle}(\psi) = (1 - \epsilon)c_{\mathrm{BM}} > 0$ in time interval $[t_1, t_2]$, where $0 \leq \epsilon \ll 1$. Then the time-evolved state ψ_τ will exhibit the same amount of backflow over the interval $[t_1 - \tau, t_2 - \tau]$. Assuming τ is sufficiently large that the two intervals are well-separated, a linear combination $\alpha\psi + \beta\psi_\tau$ will exhibit a total backflow of approximately $(|\alpha|^2 + |\beta|^2)\Delta^{(1)}_{\langle t_1,t_2\rangle}(\psi)$ across the two intervals, also assuming that cross terms between ψ and ψ_τ can be neglected. Now α and β must be chosen so that the linear combination is normalized. If ψ and ψ_τ were orthogonal, this would require $|\alpha|^2 + |\beta|^2 = 1$ and the total 2-fold backflow would be no more than $\Delta^{(1)}_{\langle t_1,t_2\rangle}(\psi)$. However, linear combinations in which some destructive interference occurs will require a normalization with $|\alpha|^2 + |\beta|^2 > 1$ whereupon the 2-fold backflow exceeds $\Delta^{(1)}_{\langle t_1,t_2\rangle}(\psi)$. Taking $\epsilon \to 0$, it is plausible that c_{BM} can be exceeded by 2-fold backflow. Although this argument leaves much to be desired, it illustrates a point that will be proved rigorously later on. In §2b, we also give a simple (and precise) argument why the existence of non-trivial backflow implies the existence of non-trivial 2-fold overflow, approaching the limit $-1 - c_{\mathrm{BM}}$.

In more detail, we show in §2 that, for all M, the classical analogue of $\Delta^{(M)}_{\langle \boldsymbol{t}_M\rangle}$ is constrained to the negative unit interval $[-1, 0]$ for classical statistical ensembles with positive momenta. Passing to quantum mechanics, a straightforward adaptation of arguments in [2,16] show that for each strictly increasing list of times $\langle \boldsymbol{t}_M\rangle$, there is a self-adjoint bounded operator $B^{(M)}_{\langle \boldsymbol{t}_M\rangle}$ on $L^2(\mathbb{R}^+, dk)$ so that

$$\Delta^{(M)}_{\langle \boldsymbol{t}_M\rangle}(\psi) = \langle \hat{\psi} | B^{(M)}_{\langle \boldsymbol{t}_M\rangle} \hat{\psi}\rangle \tag{1.3}$$

for normalized positive-momentum state $\psi \in L^2(\mathbb{R}, dx)$, where $\hat{\psi} \in L^2(\mathbb{R}^+, dk)$ is the Fourier transform of ψ, i.e. its momentum representation. It follows that the set of possible values for the total backflow is the numerical range of the operator $B^{(M)}_{\langle \boldsymbol{t}_M\rangle}$, and that the supremum and infimum of these values are, respectively, given by the maximum and minimum points of the spectrum $\sigma(B^{(M)}_{\langle \boldsymbol{t}_M\rangle})$, generalizing the original insight of [2]. The unitary equivalence of operators $B^{(M)}_{\langle \boldsymbol{t}_M\rangle}$ under simultaneous uniform translation of all times, and under simultaneous uniform dilation, implies that the maximum and minimum of $\sigma(B^{(M)}_{\langle \boldsymbol{t}_M\rangle})$ are functions of the successive ratios of successive differences of the t_j's. That is, one has bounds,

$$b^{(M)}_{\mathrm{over}}(\mathrm{srsd}\langle \boldsymbol{t}_M\rangle) \leq \Delta^{(M)}_{\langle \boldsymbol{t}_M\rangle}(\psi) \leq b^{(M)}_{\mathrm{back}}(\mathrm{srsd}\langle \boldsymbol{t}_M\rangle), \tag{1.4}$$

for all positive-momentum states ψ, where

$$\mathrm{srsd}\langle \boldsymbol{t}_M\rangle = \left(\frac{t_3 - t_2}{t_2 - t_1}, \ldots, \frac{t_{2M} - t_{2M-1}}{t_{2M-1} - t_{2M-2}}\right) \tag{1.5}$$

and $b^{(M)}_{\mathrm{back/over}} : \mathbb{R}^{2M-2}_{>0} \to \mathbb{R}$ are *backflow/overflow functions* defined so that

$$b^{(M)}_{\mathrm{back}}(\mathrm{srsd}\langle \boldsymbol{t}_M\rangle) = \max \sigma(B^{(M)}_{\langle \boldsymbol{t}_M\rangle}) \quad \text{and} \quad b^{(M)}_{\mathrm{over}}(\mathrm{srsd}\langle \boldsymbol{t}_M\rangle) = \min \sigma(B^{(M)}_{\langle \boldsymbol{t}_M\rangle}). \tag{1.6}$$

The supremum and infimum of $b^{(M)}_{\mathrm{back}}$ and $b^{(M)}_{\mathrm{over}}$ over $\mathbb{R}^{2M-2}_{>0}$ define sequences of backflow and overflow constants, $c^{(M)}_{\mathrm{back}}$ and $c^{(M)}_{\mathrm{over}}$. For $M = 1$ one has $c^{(1)}_{\mathrm{back}} = c_{\mathrm{BM}}$ and $c^{(1)}_{\mathrm{over}} = -1$.

Next, in §3, we prove two key results regarding backflow and overflow. First, we show that the backflow and overflow constants satisfy the bounds,

$$c_{\text{back}}^{(M)} \leq M c_{\text{BM}} \quad \text{and} \quad c_{\text{back}}^{(M)} \geq -1 - (M-1)c_{\text{BM}} \tag{1.7}$$

(see theorem 3.1 for the precise statement and more detail). Second, by considering the example of equal duration intervals separated by gaps of the same duration and using simple sequences of trial positive-momentum states, we prove that

$$c_{\text{back}}^{(M)} \to \infty \quad \text{and} \quad c_{\text{over}}^{(M)} \to -\infty \tag{1.8}$$

as $M \to \infty$, at least as fast as $\mathcal{O}(M^{1/4})$. See theorem 3.2 for the detailed statement.

In §4, we study various limiting cases of the backflow functions as some of their parameters are taken to zero or infinity. The main result here, theorem 4.1, provides an understanding of the relation between backflow and overflow functions for different M, and a proof that the backflow and overflow constants are monotonic in M, and obey

$$c_{\text{back}}^{(M+L)} \geq -1 - c_{\text{over}}^{(M)} \quad \text{and} \quad c_{\text{over}}^{(M+L)} \leq -1 - c_{\text{back}}^{(M)} \tag{1.9}$$

for all $M, L \in \mathbb{N}$. Various consequences are drawn. In particular it is shown that when two time intervals merge, the spectra of the corresponding backflow operators do not converge to the spectrum of the backflow operator for the merged intervals. For example, as the limit is approached, the overflow function $b_{\text{over}}^{(2)}$ tends to $-1 - c_{\text{BM}}$, while once the intervals have merged the appropriate overflow function is $b_{\text{over}}^{(1)} \equiv -1$. Thus an arbitrarily small 'recovery time' between the time intervals, during which the state exhibits backflow, is sufficient to accommodate states with maximal 2-fold overflow. Technically, the failure of spectra to converge is related to the fact that the backflow operators only converge in the strong topology rather than in norm topology. However, if one restricts attention to positive-momentum states with a fixed momentum cutoff, the maximum backflow/overflow do converge to the values for a single interval as the intervals merge. This is significant because numerical tests typically involve such a cutoff, and would yield misleading results unless the cutoff is increased as the merger is approached.

In §5, we present a numerical investigation of the situation of M equally spaced backflow periods of equal length. In particular, we aim to estimate the values of $b_{\text{back/over}}^{(M)}(1, 1, \ldots, 1)$ for $1 \leq M \leq 4$. Our method is to study the compression of the appropriate M-fold backflow operator to the $(N+1)$-dimensional subspace $V_{N,a,\delta} = \text{span}(\psi_{0,a,\delta}, \ldots, \psi_{N,a,\delta})$, where $\psi_{n,a,\delta}(p) \propto p^{n+\delta} e^{-ap}$ are normalized $L^2(\mathbb{R}^+, dp)$ vectors depending on parameters a, δ. The maximum/minimum eigenvalue $\lambda_{\text{back/over}}^{(M)}(a, \delta; N)$ of the compression can be obtained by solving a generalized eigenvalue problem relative to the Gram matrix of $\psi_{0,a,\delta}, \ldots, \psi_{N,a,\delta}$; high precision is required in the calculation because the minimum eigenvalue of the Gram matrix tends to 0 geometrically as $N \to \infty$. Fortunately, we are able to derive closed form expressions for all the matrix elements required in terms of special functions implemented in the arbitrary precision library FLINT [17,18]. The upshot is that the values $\lambda_{\text{back/over}}^{(M)}(a, \delta; N)$ are computed accurate to tens (and sometimes hundreds) of decimal places.

For choices of a and δ that we motivate, we obtain sequences $\lambda_{\text{back/over}}^{(M)}(N)$ for $1 \leq M \leq 4$ and $N \leq 500$. Up to numerical precision, these sequences converge monotonically to $b_{\text{back/over}}^{(M)}(1, 1, \ldots, 1)$ as $N \to \infty$, thus providing rigorous bounds on these quantities. The sequences converge quite slowly, but numerical acceleration techniques can be used to estimate the limiting values (albeit losing the guarantee of monotonic convergence). Our acceleration techniques assume that $\lambda_{\text{back/over}}^{(M)}(N)$ has an asymptotic expansion in powers of $N^{-1/2}$; this is supported by our results, except in the case of $\lambda_{\text{over}}^{(1)}$, which converges rapidly to $c_{\text{over}}^{(1)} = -1$.

The acceleration methods lead to conjectured upper and lower bounds for $b_{\text{back/over}}^{(M)}(1, 1, \ldots, 1)$ which are listed in tables 2 and 3. In particular, our conjectured value for c_{BM} is 0.0384506 to six significant figures. We discuss the relation to earlier calculations of [2,3] in §5c.

We also compute the normalized eigenvectors $\psi^{(M)}_{\text{back/over}}(N;\cdot) \in V_{N,a,\delta} \subset L^2(\mathbb{R}^+, dp)$ of the compressed backflow operators corresponding to eigenvalues $\lambda^{(M)}_{\text{back/over}}(N)$. For $M=1$ the overflow eigenvectors $\psi^{(1)}_{\text{over}}(N;\cdot)$ resemble Gaussians roughly peaked at $1.5N$ and with broadening width—see figure 14. We argue that this behaviour is in line with a result proved in [16], that -1 lies in the essential spectrum of the single backflow operator. The remaining eigenvectors have an oscillatory structure that becomes more complex as M increases, and appear to decay as $\mathcal{O}(p^{-3/4})$ for $p \to \infty$. The backflow eigenvectors also diverge as $p \to 0$, apparently as $\mathcal{O}(p^{-1/4})$. We present plots of $\psi^{(M)}_{\text{back/over}}(N;p)$ for $N=500$, where in most cases the wavefunctions are multiplied by a factor $p^{3/4}$ to remove the decay at large momentum, thus more clearly showing the oscillatory structure. Our results also suggest that $b^{(M)}_{\text{back}}(1,\dots,1)$ for $1 \le M \le 4$ and $b^{(M)}_{\text{over}}(1,\dots,1)$ for $2 \le M \le 4$ are isolated eigenvalues of the M-fold backflow operator. We conclude in §6 with a summary and outlook. The electronic supplementary material comprises appendices giving technical details deferred from the main text and additional plots.

2. M-fold backflow

(a) Classical statistical mechanics

Consider a classical ensemble of particles $\mathcal{C}$ of mass μ under free evolution on the line. Let the distribution of particles on phase space $\mathcal{P}=\mathbb{R}^2$ at time t be given by a probability measure ρ_t so that a randomly chosen member of the ensemble has phase space position in Borel subset $S \subseteq \mathcal{P}$ at time t with probability

$$\text{Prob}_\rho((X,P) \in S \mid t) = \rho_t(S), \tag{2.1}$$

where we write $\rho = \rho_0$ for the state at time $t=0$. The ensemble average of an observable $f \in C(\mathcal{P})$ at time t is given by $\int f\, d\rho_t = \int f \circ \tau_t \, \mathrm{d}\rho$ by Liouville's theorem, where

$$\tau_t(x,p) = \left(x + \frac{pt}{\mu}, p\right) \tag{2.2}$$

is the forwards Hamiltonian time evolution through time t. Correspondingly, we find that $\rho_t(S) = \rho(\tau_t^{-1}(S))$. If the ensemble only contains particles with non-negative momentum then one has

$$\rho(S) = \rho(S \cap (\mathbb{R} \times [0,\infty))) \tag{2.3}$$

for any Borel subset $S \subseteq \mathcal{P}$, and consequently,

$$\begin{aligned}\text{Prob}_\rho(X \in (-\infty,0) \mid t) &= \rho_t((-\infty,0)\times\mathbb{R}) \\ &= \rho(\tau_t^{-1}((-\infty,0)\times\mathbb{R})) \cap (\mathbb{R}\times[0,\infty)) \\ &= \text{Prob}_\rho\left((X,P) \in \left\{(x,p) \in \mathcal{P} : x < -\frac{pt}{\mu}, p \ge 0\right\}\right).\end{aligned} \tag{2.4}$$

The difference between the probabilities of finding a randomly chosen particle on the left-hand half-line at time t' and an earlier time t is therefore

$$\text{Prob}_\rho(X \in (-\infty,0) \mid t') - \text{Prob}_\rho(X \in (-\infty,0) \mid t) = -\text{Prob}_\rho((X,P) \in S_{t,t'}), \tag{2.5}$$

where

$$S_{t,t'} = \left\{(x,p) \in \mathcal{P} : -\frac{pt'}{\mu} \le x < -\frac{pt}{\mu}, p \ge 0\right\} \tag{2.6}$$

for any $t' > t$. Note that we may replace $p \ge 0$ by $p > 0$ in the formula $S_{t,t'}$ without loss because $S_{t,t'} \cap (\mathbb{R}\times\{0\}) = \emptyset$. Accordingly, $-\rho(S_{t,t'})$ measures the probability backflow between times t and t'; as it is clearly non-positive, we see that there is no classical backflow.

Now consider adding together the backflow for a set of disjoint time intervals. Specifically, given $M \in \mathbb{N}$ and times $t_1 < t_2 < \cdots < t_{2M-1} < t_{2M}$, the total amount of probability backflow is given by

$$\begin{aligned}\Delta^{(M)}_{\text{classical}}(\rho) &:= \sum_{j=1}^{M} (\text{Prob}_\rho(X \in (-\infty, 0) \mid t_{2j}) - \text{Prob}_\rho(X \in (-\infty, 0) \mid t_{2j-1})) \\ &= -\sum_{j=1}^{M} \text{Prob}_\rho(X \in S_{t_{2j-1}, t_{2j}}) = -\text{Prob}_\rho\left(X \in \bigcup_{j=1}^{M} S_{t_{2j-1}, t_{2j}}\right), \end{aligned} \tag{2.7}$$

because the sets $S_{t_{2j-1},t_{2j}}$ are disjoint for distinct j.

It follows that, for a classical ensemble with non-negative momentum, the total amount of probability backflow over multiple disjoint time periods is bounded by

$$-1 \leq \Delta^{(M)}_{\text{classical}}(\rho) \leq 0, \tag{2.8}$$

for every M. In particular, a classical ensemble cannot exhibit positive probability backflow, and the probability transfer in the forward direction is bounded by unity. By contrast, it is well known that quantum particles can exhibit backflow over a single time interval, thus violating the upper bound in the analogue of equation (2.8). One of the main results of this paper is to see that the violation increases with M, and that the lower bound of equation (2.8) is also violated in quantum theory for $M \geq 2$.

We remark that if one drops the restriction $p > 0$ then a similar argument to the above shows that $\Delta^{(M)}_{\text{classical}}(\rho)$ can be written as a difference of two probabilities and therefore lies in $[-1, 1]$. Thus, while backflow is certainly possible (but unsurprising) in this case, classical overflow is always forbidden.

(b) Quantum mechanics

We turn to the quantum case, using units in which $\hbar = 1$. Consider the motion of a free quantum particle of mass μ with normalized state vector $\psi_t \in L^2(\mathbb{R}^+)$ at time t, whose dynamics are governed by the free Schrödinger equation:

$$i\partial_t \psi_t = -\frac{1}{2\mu}\partial_x^2 \psi_t \tag{2.9}$$

and initial condition $\psi_0 = \psi$, so $\psi_t = e^{-ip^2 t}\psi$, where $p = -i\partial_x$ and we have chosen units so that $\mu = \frac{1}{2}$, as we shall do from now on for simplicity. The states with non-negative momentum form the subspace

$$\mathcal{H}_+ = \{\psi \in L^2(\mathbb{R}, \mathrm{d}x) : \text{supp}\, \hat{\psi} \subseteq [0, \infty)\}, \tag{2.10}$$

where

$$\hat{\psi}(p) = \frac{1}{\sqrt{2\pi}} \int_{\mathbb{R}} \mathrm{d}x\, \mathrm{e}^{-\mathrm{i}px} \psi(x) \tag{2.11}$$

is the Fourier transform of ψ.

Let $t_1 < t_2$. The probability backflow exhibited by the normalized $t = 0$ state ψ between times t_1 and t_2 is quantified by

$$\Delta_{\langle t_1, t_2 \rangle}(\psi) := \text{Prob}_\psi(X < 0 \mid t_2) - \text{Prob}_\psi(X < 0 \mid t_1), \tag{2.12}$$

where $\text{Prob}_\psi(X \in S \mid t) = \int_S dx\, |\psi_t(x)|^2$ is the probability of measuring the position of the particle to lie in S at time t. There are simple examples of states $\psi \in \mathcal{H}_+$ for which $\Delta_{\langle t_1, t_2 \rangle}(\psi) > 0$, showing that quantum mechanical particles can exhibit non-trivial backflow (e.g. [19]) whereas the classical backflow quantity for particles always lies in $[-1, 0]$.

We are interested in the range of values assumed by $\Delta_{\langle t_1, t_2 \rangle}(\psi)$ as ψ varies over normalized states of $\mathcal{H}_+$. As a difference of probabilities, its range is contained in $[-1, 1]$. Moreover, because

$\mathcal{H}_+$ is invariant under both the free time evolution and dilations, the range is invariant under $\langle t_1, t_2\rangle \mapsto \langle t_1+\tau, t_2+\tau\rangle$ and $\langle t_1, t_2\rangle \mapsto \langle \lambda t_1, \lambda t_2\rangle$ for all $\tau \in \mathbb{R}$ and all $\lambda > 0$. It follows that the range is independent of both t_1 and t_2, provided $t_1 < t_2$, as was observed by Bracken & Melloy [2]. As noted in [16], Dollard's lemma (lemma 4 of [20]) shows that $\mathrm{Prob}_\psi(X < 0 \mid t_1) \to 1$ as $t_1 \to -\infty$ and $\mathrm{Prob}_\psi(X < 0 \mid t_2) \to 0$ as $t_2 \to +\infty$ for any fixed $\psi \in \mathcal{H}_+$, thus giving $\Delta_{\langle t_1,t_2\rangle}(\psi) \to -1$ when both limits are taken. Thus -1 belongs to the closure of the range of $\Delta_{\langle t_1,t_2\rangle}$ for any $t_1 < t_2$.

More detailed information can be found by reformulating backflow in terms of operators. For normalized $\psi \in \mathcal{H}_+$, a calculation owing to Bracken & Melloy [2] gives $\Delta_{\langle t_1,t_2\rangle}(\psi)$ as a quadratic form:

$$\Delta_{\langle t_1,t_2\rangle}(\psi) = -\frac{1}{2\pi i}\int_0^\infty \mathrm{d}p \int_0^\infty \mathrm{d}q \frac{\mathrm{e}^{\mathrm{i}(p^2-q^2)t_2} - e^{i(p^2-q^2)t_1}}{p-q}\hat{\psi}^*(p)\hat{\psi}(q), \tag{2.13}$$

which can be written as

$$\Delta_{\langle t_1,t_2\rangle}(\psi) = \langle \hat{\psi} | B_{\langle t_1,t_2\rangle}\hat{\psi}\rangle. \tag{2.14}$$

Here, the operator $B_{\langle t_1,t_2\rangle}$ on $L^2(\mathbb{R}^+)$ has the following properties, which are established in §A of the electronic supplementary material, drawing on arguments in [4].

Theorem 2.1. *For any $t_1 < t_2$, $B_{\langle t_1,t_2\rangle}$ is a bounded self-adjoint operator with $||B_{\langle t_1,t_2\rangle}|| = 1$. There is a unitary equivalence between $B_{\langle t_1,t_2\rangle}$ and the operator $C \in \mathcal{B}(L^2(\mathbb{R}^+, dq))$ with action*

$$(C\varphi)(p) = -\frac{1}{2\pi}\int_0^\infty \mathrm{d}q \frac{\sin(p-q)}{p-q}\left[\left(\frac{p}{q}\right)^{1/4} + \left(\frac{p}{q}\right)^{-1/4}\right]\varphi(q) \tag{2.15}$$

on $\varphi \in L^2(\mathbb{R}^+, dq)$, where equation (2.15) holds pointwise almost everywhere on $\mathbb{R}^+$. The map $(t_1, t_2) \mapsto B_{\langle t_1,t_2\rangle}$ is strongly continuous on $\{(t_1, t_2) \in \mathbb{R}^2 : t_1 < t_2\}$.

The unitary equivalence in theorem 2.1 is a combination of translations, scale transformation and a change of variables. It follows from equation (2.14) that the range of $\Delta_{\langle t_1,t_2\rangle}(\psi)$, as ψ varies over the normalized elements of $\mathcal{H}_+$, is the *numerical range* of the operator $B_{\langle t_1,t_2\rangle}$. We recall the definition and main properties of numerical range (see §9.3 of [21]).

Definition 2.2. Let A be a bounded self-adjoint operator on a Hilbert space $\mathcal{H}$. The *numerical range* $\mathcal{N}(A) \subset \mathbb{R}$ of A is given by

$$\mathcal{N}(A) = \left\{ \frac{\langle\phi|A\phi\rangle}{\langle\phi|\phi\rangle} \,\middle|\, \phi \in \mathcal{H} \setminus \{0\} \right\}. \tag{2.16}$$

One has $\mathcal{N}(A) = \mathcal{N}(UAU^*)$ for any unitary $U \in \mathcal{B}(\mathcal{H})$, and

$$\sigma(A) \subseteq \overline{\mathcal{N}(A)} = \mathrm{Conv}\,\sigma(A), \tag{2.17}$$

where $\bar{\cdot}$ denotes topological closure and Conv the convex hull. In particular $\sigma(A)$ and $\mathcal{N}(A)$ have the same supremum and infimum.

It follows immediately that, for all $t_1 < t_2$,

$$\overline{\mathcal{N}(B_{\langle t_1,t_2\rangle})} = \mathrm{Conv}\,\sigma(C) \subseteq [-1, 1], \tag{2.18}$$

using $||C|| = 1$. We have already noted that $-1 \in \overline{\mathcal{N}(B_{\langle t_1,t_2\rangle})}$. Defining the *Bracken–Melloy constant* as the largest spectral point of C,

$$c_{\mathrm{BM}} = \sup\sigma(C) = \max\sigma(C), \tag{2.19}$$

the possible values of the backflow $\Delta_{\langle t_1,t_2\rangle}(\psi)$ obey

$$-1 \le \Delta_{\langle t_1,t_2\rangle}(\psi) \le c_{\mathrm{BM}} \tag{2.20}$$

for all normalized $\psi \in \mathcal{H}_+$.

These ideas are readily generalized to consider the total backflow over $M \ge 1$ disjoint time intervals $[t_{2j-1}, t_{2j}]$ for $1 \le j \le M$, which can be represented by a list $\langle \boldsymbol{t}_M\rangle = \langle t_1, \ldots, t_{2M}\rangle$ in strictly increasing order.

Definition 2.3. For positive integer M, let

$$\mathcal{T}_M = \left\{ \langle \boldsymbol{t}_M \rangle = \langle t_1, \ldots, t_{2M} \rangle | t_1 < t_2 < \cdots < t_{2M-1} < t_{2M} \right\}. \tag{2.21}$$

The total probability backflow exhibited by the time-zero state $\psi \in L^2(\mathbb{R}, \mathrm{d}x)$ over the intervals parameterized by $\langle \boldsymbol{t}_M \rangle \in \mathcal{T}_M$ is defined as

$$\Delta^{(M)}_{\langle \boldsymbol{t}_M \rangle}(\psi) := \sum_{j=1}^{M} (\mathrm{Prob}_\psi(X < 0 | t = t_{2j}) - \mathrm{Prob}_\psi(X < 0 | t = t_{2j-1})), \tag{2.22}$$

so that, for example, $\Delta^{(1)}_{\langle t_1 \rangle}(\psi) = \Delta_{\langle t_1, t_2 \rangle}(\psi)$.

For normalized $\psi \in \mathcal{H}_+$, one has

$$\Delta^{(M)}_{\langle \boldsymbol{t}_M \rangle}(\psi) = \langle \hat{\psi} | B^{(M)}_{\langle \boldsymbol{t}_M \rangle} \hat{\psi} \rangle, \tag{2.23}$$

where the *M-fold backflow operator*

$$B^{(M)}_{\langle \boldsymbol{t}_M \rangle} = \sum_{j=1}^{M} B_{\langle t_{2j}, t_{2j-1} \rangle} \tag{2.24}$$

is a bounded self-adjoint operator on $L^2(\mathbb{R}^+, \mathrm{d}q)$ acting as

$$(B^{(M)}_{\langle \boldsymbol{t}_M \rangle} \phi)(p) = -\frac{1}{2\pi i} \int_0^\infty \mathrm{d}q \sum_{k=1}^{M} \frac{e^{i(p^2-q^2)t_{2k}} - \mathrm{e}^{\mathrm{i}(p^2-q^2)t_{2k-1}}}{p-q} \phi(q). \tag{2.25}$$

In the same way as before, the set of possible values taken by $\Delta^{(M)}_{\langle \boldsymbol{t}_M \rangle}(\psi)$ for normalized $\psi \in \mathcal{H}_+$ is the numerical range of $B^{(M)}_{\langle \boldsymbol{t}_M \rangle}$ and can be studied via its spectrum. As before, if $\Delta^{(M)}_{\langle \boldsymbol{t}_M \rangle}(\psi) > 0$, we say that the state exhibits QB. We shall also investigate states $\psi \in \mathcal{H}_+$ for which $\Delta^{(M)}_{\langle \boldsymbol{t}_M \rangle}(\psi) < -1$ for $M \geq 2$, a phenomenon we call *quantum overflow*. As noted in the introduction, overflow would also be interesting in the situation where the positive-momentum assumption is dropped, and perhaps exhibits a greater quantum advantage in that case, but this is not pursued here.

The following straightforward argument shows the existence of states exhibiting quantum overflow with $M = 2$. Fix $t_1 < t_2$ and suppose $\psi \in \mathcal{H}_+$ is such that $\Delta^{(1)}_{\langle t_1, t_2 \rangle}(\psi) = \lambda > 0$, i.e. there is non-trivial backflow between t_1 and t_2. Taking $T > \max(|t_1|, |t_2|)$, one can write the total backflow over $[-T, t_1] \cup [t_2, T]$ as

$$\Delta^{(2)}_{\langle -T, t_1, t_2, T \rangle}(\psi) = \Delta^{(1)}_{\langle -T, T \rangle}(\psi) - \Delta^{(1)}_{\langle t_1, t_2 \rangle}(\psi). \tag{2.26}$$

For any fixed $\epsilon \in (0, \lambda)$, one can find T sufficiently large such that $\Delta^{(1)}_{\langle -T, T \rangle}(\psi) < -1 + \epsilon$, because Dollard's lemma [20] implies that $\Delta^{(1)}_{\langle -T, T \rangle}(\psi) \to -1$ as $T \to \infty$. It follows that

$$\Delta^{(2)}_{\langle -T, t_1, t_2, T \rangle}(\psi) < -1 - \lambda + \epsilon < -1, \tag{2.27}$$

showing that the state ψ exhibits quantum overflow on $[-T, t_1] \cup [t_2, T]$. As ψ can be chosen to make λ arbitrarily close to c_{BM} and ϵ could be chosen arbitrarily small, this already shows that 2-fold overflow can approach $-1 - c_{\mathrm{BM}}$ over suitable intervals. In this example, we chose the time interval after fixing the state, without any control on the size of T. However, in §3b, we shall consider M equally spaced intervals of equal width, and show that the total M-fold overflow can be made unboundedly negative as M increases, and similarly that the M-fold backflow can be made unboundedly positive as M increases.

The invariance of $\mathcal{H}_+$ under time evolution and dilations does not completely fix $\mathcal{N}(B^{(M)}_{\langle \boldsymbol{t}_M \rangle})$ if $M > 1$. However, time translation invariance shows that $\mathcal{N}(B^{(M)}_{\langle \boldsymbol{t}_M \rangle})$ is a function of the successive differences $(t_2 - t_1, t_3 - t_2, \ldots, t_{2M} - t_{2M-1})$, and the scaling invariance shows that it may be

expressed in terms of successive ratios of these differences. For each $M > 1$, then, there are *backflow and overflow functions* $b^{(M)}_{\text{back/over}} : \mathbb{R}^{2M-2}_{>0} \to \mathbb{R}$ (writing $\mathbb{R}^k_{>0} = (0,\infty)^{\times k}$) so that

$$\sup \mathcal{N}(B^{(M)}_{\langle \boldsymbol{t}_M\rangle}) = b^{(M)}_{\text{back}}\left(\frac{t_3 - t_2}{t_2 - t_1}, \ldots, \frac{t_{2M} - t_{2M-1}}{t_{2M-1} - t_{2M-2}}\right) = b^{(M)}_{\text{back}}(\text{srsd}\langle \boldsymbol{t}_M\rangle) \tag{2.28}$$

and

$$\inf \mathcal{N}(B^{(M)}_{\langle \boldsymbol{t}_M\rangle}) = b^{(M)}_{\text{over}}\left(\frac{t_3 - t_2}{t_2 - t_1}, \ldots, \frac{t_{2M} - t_{2M-1}}{t_{2M-1} - t_{2M-2}}\right) = b^{(M)}_{\text{over}}(\text{srsd}\langle \boldsymbol{t}_M\rangle), \tag{2.29}$$

where srsd is the operation of forming the sequence of successive ratios of successive differences. By convention, we write $b^{(1)}_{\text{back}} = c_{\text{BM}}$, $b^{(1)}_{\text{over}} = -1$, and srsd maps any element of $\mathcal{T}_1$ to the empty list. As we now describe, the backflow and overflow functions are semicontinuous.

Lemma 2.4. *For each $M > 1$, the functions $b^{(M)}_{\text{back/over}}$ are lower/upper semicontinuous on $\mathbb{R}^{2M-2}_{>0}$. That is, for all $u_0 \in \mathbb{R}^{2M-2}_{>0}$, one has*

$$\liminf_{u\to u_0} b^{(M)}_{\text{back}}(u) \geq b^{(M)}_{\text{back}}(u_0) \quad \text{and} \quad \limsup_{u\to u_0} b^{(M)}_{\text{over}}(u) \leq b^{(M)}_{\text{over}}(u_0), \tag{2.30}$$

as $u \to u_0$ in $\mathbb{R}^{2M-2}_{>0}$.

Proof. The function $\langle \boldsymbol{t}_M\rangle \mapsto B^{(M)}_{\langle \boldsymbol{t}_M\rangle}$ is strongly continuous on $\mathcal{T}_M$ owing to equation (2.24) and theorem 2.1, so for each normalized $\phi \in L^2(\mathbb{R}^+, dq)$, $\langle \boldsymbol{t}_M\rangle \mapsto \langle \phi | B^{(M)}_{\langle \boldsymbol{t}_M\rangle}\phi\rangle$ is continuous on $\mathcal{T}_M$. As $\langle \boldsymbol{t}_M\rangle \mapsto \sup \mathcal{N}(B^{(M)}_{\langle \boldsymbol{t}_M\rangle}) = b^{(M)}_{\text{back}}(\text{srsd}\langle \boldsymbol{t}_M\rangle)$ is the pointwise supremum over ϕ of a family of continuous functions, it is lower semicontinuous (e.g. Chapter 2 of [22]). Fixing $\tau > 0$, it follows that $b^{(M)}_{\text{back}} \circ \text{srsd}$ is lower semicontinuous on the subset $\{\langle 0, \tau, t_3, \ldots, t_{2M}\rangle \in \mathcal{T}_M\}$ (in the relative topology). As this subset is mapped homeomorphically to $\mathbb{R}^{2M-2}_{>0}$ by srsd, we conclude that $b^{(M)}_{\text{back}}$ is lower semicontinuous on $\mathbb{R}^{2M-2}_{>0}$. The proof for the overflow functions is similar. ∎

We also introduce sequences of backflow and overflow constants, by

$$c^{(M)}_{\text{back}} = \sup_{\mathbb{R}^{2M-2}_{>0}} b^{(M)}_{\text{back}} \quad \text{and} \quad c^{(M)}_{\text{over}} = \inf_{\mathbb{R}^{2M-2}_{>0}} b^{(M)}_{\text{over}} \tag{2.31}$$

for $M \geq 1$, in which the Bracken–Melloy constant appears as the first backflow constant: $c_{\text{BM}} = c^{(1)}_{\text{back}}$, while the first overflow constant is $c^{(1)}_{\text{over}} = -1$. Just as with c_{BM}, the functions $b^{(M)}_{\text{back/over}}$ and constants $c^{(M)}_{\text{back/over}}$ are quantities that are fixed by the free quantum dynamics on the line. However, as the $b^{(M)}_{\text{back/over}}$ are dimensionless functions of dimensionless variables, they are manifestly independent of Planck's constant. In the remainder of this paper, we shall initiate the study of these functions and constants using both analytical and numerical methods, starting by considering the spectrum of the operators $B^{(M)}_{\langle \boldsymbol{t}_M\rangle}$ for $\langle \boldsymbol{t}_M\rangle \in \mathcal{T}_M$.

3. The spectrum of M-fold backflow operators

(a) Bounds on the spectrum

Our aim in this section is to obtain estimates on $\sigma(B^{(M)}_{\langle \boldsymbol{t}_M\rangle})$ for a variety of $\langle \boldsymbol{t}_M\rangle \in \mathcal{T}_M$. The simplest estimate arises from the triangle inequality: since $||B_{\langle t_1,t_2\rangle}|| = 1$ for all $t_1 < t_2$, we have from equation (2.24) that $||B^{(M)}_{\langle \boldsymbol{t}_M\rangle}|| \leq M$ and consequently $\sigma(B^{(M)}_{\langle \boldsymbol{t}_M\rangle}) \subseteq [-M, M]$ for all $\langle \boldsymbol{t}_M\rangle \in \mathcal{T}_M$ and $M \geq 1$.

To get a better estimate of the upper bound on the spectrum, we note that any sum of self-adjoint bounded operators obeys

$$\sup\sigma\left(\sum_{j=1}^{M}A_j\right)\leq\sum_{j=1}^{M}\sup\sigma(A_j) \tag{3.1}$$

and therefore

$$\sup\sigma(B^{(M)}_{\langle \boldsymbol{t}_M\rangle})\leq\sum_{j=1}^{M}\sup\sigma(B_{\langle t_{2j-1},t_{2j}\rangle})=Mc_{\mathrm{BM}}. \tag{3.2}$$

To get a lower bound on the spectrum, it is convenient to rewrite $\Delta^{(M)}_{\langle \boldsymbol{t}_M\rangle}(\psi)$ as

$$\begin{aligned}\Delta^{(M)}_{\langle \boldsymbol{t}_M\rangle}(\psi)&=\mathrm{Prob}_\psi(X<0|t=t_{2M})-\mathrm{Prob}_\psi(X<0|t=t_1)\\&\quad-\sum_{j=1}^{M-1}(\mathrm{Prob}_\psi(X<0|t=t_{2j+1})-\mathrm{Prob}_\psi(X<0|t=t_{2j})),\end{aligned} \tag{3.3}$$

from which it follows that

$$B^{(M)}_{\langle \boldsymbol{t}_M\rangle}=B_{\langle t_1,t_{2M}\rangle}-B^{(M-1)}_{\langle t_2,\ldots,t_{2M-1}\rangle}. \tag{3.4}$$

Iterating, one obtains the formula

$$B^{(M)}_{\langle \boldsymbol{t}_M\rangle}=\sum_{j=1}^{M}(-1)^{j-1}B_{\langle t_j,t_{2M-j+1}\rangle}, \tag{3.5}$$

which will be used later on.

Returning to equation (3.4), an analogue of equation (3.1) gives

$$\begin{aligned}\inf\sigma(B^{(M)}_{\langle \boldsymbol{t}_M\rangle})&\geq\inf\sigma(B_{\langle t_1,t_{2M}\rangle})+\inf\sigma(-B^{(M-1)}_{\langle t_2,\ldots,t_{2M-1}\rangle})\\&=-1-\sup\sigma(B^{(M-1)}_{\langle t_2,\ldots,t_{2M-1}\rangle})\\&\geq-1-(M-1)c_{\mathrm{BM}},\end{aligned} \tag{3.6}$$

where we have used equation (3.2). Summarizing, we have shown the following:

Theorem 3.1. *For any $M\in\mathbb{N}$ and $\langle \boldsymbol{t}_M\rangle\in\mathcal{T}_M$, the spectrum of $B^{(M)}_{\langle \boldsymbol{t}_M\rangle}$ satisfies*

$$\sigma(B^{(M)}_{\langle \boldsymbol{t}_M\rangle})\subseteq[-1-(M-1)c_{\mathrm{BM}},Mc_{\mathrm{BM}}]. \tag{3.7}$$

Thus one has bounds

$$b^{(M)}_{\mathrm{back}}(u_1,\ldots,u_{2M-2})\leq c^{(M)}_{\mathrm{back}}\leq Mc_{\mathrm{BM}} \tag{3.8}$$

and

$$b^{(M)}_{\mathrm{over}}(u_1,\ldots,u_{2M-2})\geq c^{(M)}_{\mathrm{over}}\geq-1-(M-1)c_{\mathrm{BM}}, \tag{3.9}$$

for all $(u_1,\ldots,u_{2M-2})\in\mathbb{R}^{2M-2}_{>0}$.

Theorem 3.1 shows that $c^{(M)}_{\mathrm{back/over}}$ do not grow faster than linearly in M, but does not answer the question of whether they grow at all. In the following subsections we prove rigorously that for a particular class of backflow operators, both the infimum and supremum of $\sigma(B^{(M)}_{\langle \boldsymbol{t}_M\rangle})$ tend to $\pm\infty$ as $M\to\infty$ at least as fast as $\mathcal{O}(M^{1/4})$. This is in stark contrast to the classical case where, irrespective of the number of disjoint backflow intervals, the total backflow always lies in $[-1,0]$. The rigorous results presented will be supplemented by a numerical investigation for values of $1\leq M\leq 4$ which clearly indicate monotonicity of the infimum and supremum of $\sigma(B^{(M)}_{\langle \boldsymbol{t}_M\rangle})$.

(b) Unbounded M-fold backflow and overflow as $M \to \infty$

In this subsection we show that $c^{(M)}_{\text{back}}$ and $-c^{(M)}_{\text{over}}$ grow unboundedly with M, by considering the M-fold backflow operator corresponding to M backflow periods of equal duration, separated by $M-1$ intervals of the same duration. Specifically, for $M \in \mathbb{N}$ and fixed $T > 0$, consider the M-fold backflow problem for the times

$$\langle \boldsymbol{t}_M \rangle = \left\langle -T\frac{2M-1}{2}, -T\frac{2M-3}{2}, \ldots, -\frac{T}{2}, \frac{T}{2}, \ldots, T\frac{2M-1}{2} \right\rangle, \tag{3.10}$$

for which the total backflow is bounded between $b^{(M)}_{\text{over}}(1,\ldots,1)$ and $b^{(M)}_{\text{back}}(1,\ldots,1)$. Note that $b^{(M)}_{\text{over}}(1,\ldots,1)$ and $b^{(M)}_{\text{back}}(1,\ldots,1)$ are invariant under the choice of $T > 0$. One can write the associated M-fold backflow operator $B^{(M)}_{\langle \boldsymbol{t}_M \rangle}$ as

$$B^{(M)}_{\langle \boldsymbol{t}_M \rangle} = \sum_{j=1}^{M} (-1)^{j-1} B^{(1)}_{\langle -T(j-1/2), T(j-1/2) \rangle}, \tag{3.11}$$

using equation (3.5). Each of the $B^{(1)}_{\langle -T(j-1/2), T(j-1/2) \rangle}$ operators has the closed form

$$(B^{(1)}_{\langle -T(j-1/2), T(j-1/2) \rangle}\phi)(k) = -\frac{1}{\pi}\int_0^\infty \mathrm{d}l \frac{\sin(T(j-1/2)(k^2-l^2))}{k-l}\phi(l). \tag{3.12}$$

Let $U : L^2(\mathbb{R}^+, dk) \to L^2(\mathbb{R}^+, dp)$ be the unitary implementing the change of variables $p = k^2T/2$, $(U\phi)(p) = (2pT)^{-1/4}\phi(\sqrt{2p/T})$, so that $U^* B^{(1)}_{\langle -T/2, T/2 \rangle} U = C$ is the operator defined in equation (2.15). Then it is easily seen, by use of the identity

$$\sum_{j=1}^{M} (-1)^{M-j} \sin(2(j-1/2)(p-q)) = \frac{\sin 2M(p-q)}{2\cos(p-q)}, \tag{3.13}$$

that the operator $C^{(M)} = U^* B^{(M)}_{\langle \boldsymbol{t}_M \rangle} U \in \mathcal{B}(L^2(\mathbb{R}^+, dq))$ is independent of T and has the action

$$(C^{(M)}\varphi)(p) = -\frac{1}{4\pi}\int_0^\infty \mathrm{d}q \frac{\sin(2M[p-q])}{(p-q)\cos(p-q)} \left[\left(\frac{p}{q}\right)^{1/4} + \left(\frac{p}{q}\right)^{-1/4} \right] \varphi(q). \tag{3.14}$$

The following theorem shows that the suprema and infima of $\mathcal{N}(B^{(M)}_{\langle \boldsymbol{t}_M \rangle}) = \mathcal{N}(C^{(M)})$ grow arbitrarily large in magnitude with M at least as fast as $\mathcal{O}(M^{1/4})$.

Theorem 3.2. *For $M \in \mathbb{N}$, let $C^{(M)} \in \mathcal{B}(L^2(\mathbb{R}^+, dq))$ be the backflow operator defined in equation (3.14) describing M backflow periods of unit duration separated by $M-1$ periods of unit duration. Then there is a constant $k > 0$ so that*

$$\sup \sigma(C^{(M)}) \geq k M^{1/4} \tag{3.15}$$

for all positive even M, and furthermore,

$$\liminf_{M\to\infty} M^{-1/4} \sup \sigma(C^{(M)}) \geq k > 0 \quad \text{and} \quad \limsup_{M\to\infty} M^{-1/4} \inf \sigma(C^{(M)}) \leq -k < 0, \tag{3.16}$$

where the limits are taken over all $M \in \mathbb{N}$.

Proof. For even $M \in \mathbb{N}$ and $\epsilon \in (0, \frac{\pi}{6}]$, define the intervals $\mathcal{I}_0, \mathcal{I}_1 \subseteq \mathbb{R}$ by

$$\mathcal{I}_0 = \left[0, \frac{\epsilon}{M}\right] \quad \text{and} \quad \mathcal{I}_1 = \left[\frac{\pi}{2} - \frac{\epsilon}{2M}, \frac{\pi}{2} + \frac{\epsilon}{2M}\right] \tag{3.17}$$

and associated normalized $\psi_M \in L^2(\mathbb{R}^+, dq)$ by

$$\psi_M(q) = \begin{cases} \sqrt{\dfrac{M}{2\epsilon}}, & q \in \mathcal{I}_0 \cup \mathcal{I}_1, \\ 0, & \text{otherwise.} \end{cases} \tag{3.18}$$

The supremum of the spectrum is estimated using the bound $\sup\sigma(C^{(M)}) \geq \langle\psi_M|C^{(M)}\psi_M\rangle$. This is computed in the electronic supplementary material, §B, which also details the proofs of equations (3.15) and (3.16). ■

Note that equations (3.16) are poor bounds on the spectra of $C^{(M)}$. However, they show that simple states can deliver arbitrarily large amounts of backflow and overflow. Theorem 3.2 has an immediate corollary relating to the asymptotics of the backflow and overflow constants.

Corollary 3.3. *Let $c^{(M)}_{\mathrm{back}}$ and $c^{(M)}_{\mathrm{over}}$ be the M-fold backflow and overflow constants defined in equation (2.31). Then*

$$\liminf_{M\to\infty} M^{-1/4} c^{(M)}_{\mathrm{back}} > 0 \quad \text{and} \quad \limsup_{M\to\infty} M^{-1/4} c^{(M)}_{\mathrm{over}} < 0. \tag{3.19}$$

Proof. Since $C^{(M)}$ is unitarily equivalent to $B^{(M)}_{\langle \boldsymbol{t}_M(T)\rangle'}$, we find that

$$\sup\sigma(C^{(M)}) = b^{(M)}_{\mathrm{back}}(1,\ldots,1) \leq c^{(M)}_{\mathrm{back}} \quad \text{and} \quad \inf\sigma(C^{(M)}) = b^{(M)}_{\mathrm{over}}(1,\ldots,1) \geq c^{(M)}_{\mathrm{over}}. \tag{3.20}$$

The result follows on multiplying each inequality by $M^{-1/4}$ and employing lemma 3.2, together with elementary properties of lim sup and lim inf. ■

Theorem 3.2 and corollary 3.3 demonstrate the unboundedness of the QB and overflow effects as $M \to \infty$. In §5, we find numerical estimates of the spectral extrema for M equally spaced intervals of equal width, with $2 \leq M \leq 4$, showing in particular that

$$\sup(C^{(M)}) > c_{\mathrm{BM}} \quad \text{and} \quad \inf(C^{(M)}) < -1, \tag{3.21}$$

and further give numerical evidence for lower bounds on $c^{(M)}_{\mathrm{back}}$ as well as plots of vectors in $L^2(\mathbb{R}^+, dp)$ exhibiting backflow and overflow.

4. Limiting cases and monotonicity of the backflow constants

In lemma 2.4 we saw that the M-fold backflow and overflow functions are semicontinuous for limits taken within $\mathbb{R}^{2M-2}_{>}$. We now consider certain limiting cases, which show how backflow and overflow functions with different numbers of parameters are related and establish monotonicity properties of the backflow constants.

Theorem 4.1. *Let $M \in \mathbb{N}$ and $j, k \in \mathbb{N}_0$ so that $j + k = 2L$ is even and positive. Consider any $u \in \mathbb{R}^{(2M-2)}_{>}$ and any sequences $(v_n)_{n\in\mathbb{N}}$ in $\mathbb{R}^j_>$ and $(w_n)_{n\in\mathbb{N}}$ in $\mathbb{R}^k_>$ whose last and first components obey $v_{n,j} \to 0$ and $w_{n,1} \to \infty$. (In the case $M = 1$ one omits u; similarly, in the cases $j = 0$ resp., $k = 0$ one omits v resp., w.)*

If j (and hence also k) is even, then

$$\liminf_n b^{(M+L)}_{\mathrm{back}}(v_n, u, w_n) \geq b^{(M)}_{\mathrm{back}}(u) \quad \text{and} \quad \limsup_n b^{(M+L)}_{\mathrm{over}}(v_n, u, w_n) \leq b^{(M)}_{\mathrm{over}}(u), \tag{4.1}$$

where we use the shorthand notation $(v, u, w) = (v_1, \ldots, v_j, u_1, \ldots, u_{2M-2}, w_1, \ldots, w_k)$.

On the other hand, if j (and hence also k) is odd, then

$$\liminf_n b^{(M+L)}_{\mathrm{back}}(v_n, u, w_n) \geq -1 - b^{(M)}_{\mathrm{over}}(u) \quad \text{and} \quad \limsup_n b^{(M+L)}_{\mathrm{over}}(v_n, u, w_n) \leq -1 - b^{(M)}_{\mathrm{back}}(u). \tag{4.2}$$

Consequently, the sequence of backflow constants $c^{(M)}_{\mathrm{back}}$ is non-decreasing, and the sequence of overflow constants $c^{(M)}_{\mathrm{over}}$ is non-increasing; moreover, $c^{(M+L)}_{\mathrm{back}} \geq -1 - c^{(M)}_{\mathrm{over}}$ and $c^{(M+L)}_{\mathrm{over}} \leq -1 - c^{(M)}_{\mathrm{back}}$ for all $L \in \mathbb{N}$.

We remark that the result holds also, with the same proof, if the sequences v_n and w_n are replaced by nets. The proof can be found in the electronic supplementary material, §D.

Theorem 4.1 has a number of consequences. First, the bound $c^{(2)}_{\text{over}} \leq -1 - c^{(1)}_{\text{back}}$ can be combined with equation (3.9) to give the sharp value

$$c^{(2)}_{\text{over}} = -1 - c_{\text{BM}}. \tag{4.3}$$

Second, as the overflow constants are non-increasing, we see that for every $M \geq 2$ and $\epsilon > 0$ there exists $\langle \boldsymbol{t}_M \rangle \in \mathcal{T}_M$ and $\psi \in \mathcal{H}_+$ so that

$$\Delta^{(M)}_{\langle \boldsymbol{t}_M \rangle}(\psi) \leq -1 - c_{\text{BM}} + \epsilon, \tag{4.4}$$

which (taking $0 < \epsilon < c_{\text{BM}}$) provides another proof of the existence of overflow states for any $M \geq 2$. Similarly, we may deduce that there are backflow states for every $M \in \mathbb{N}$.

Third, the proof of theorem 4.1 can be modified slightly to give the following result (many other variations are possible) which may be useful for further studies. The notation Li will be explained after the statement, which is also proved in the electronic supplementary material, §D.

Theorem 4.2. *For $M \in \mathbb{N}$ and $\langle \boldsymbol{t}_M \rangle \in \mathcal{T}_M$, one has*

$$-1 - \mathcal{N}(B^{(M)}_{\langle \boldsymbol{t}_M \rangle}) \subseteq \text{Li}_{T_\pm \to \pm\infty} \mathcal{N}(B^{(M+1)}_{\langle T_-, \boldsymbol{t}_M, T_+ \rangle}) \tag{4.5}$$

and

$$\mathcal{N}(B^{(M)}_{\langle \boldsymbol{t}_M \rangle}) \subseteq \text{Li}_{\substack{T, T' \to -\infty \\ T < T'}} \mathcal{N}(B^{(M+1)}_{\langle T, T', \boldsymbol{t}_M \rangle}). \tag{4.6}$$

Here, Li denotes the *Painlevé–Kuratowski lower closed limit*, e.g. chapter 29 of [23] and chapter 5 of [24], defined as follows.

Definition 4.3. Given a net of sets $(A_\alpha)_{\alpha \in I}$ in a topological space X, where I is a directed set, $\text{Li}\, A_\alpha \subseteq X$ is the set of points $p \in X$ with the property that, for every neighbourhood N of p, there exists $\alpha_0 \in I$ with $A_\alpha \cap N \neq \emptyset$ for all $\alpha > \alpha_0$, i.e. every neighbourhood of p is eventually intersected by A_α.

A fourth consequence of theorem 4.1 is that it provides an understanding of how the spectrum of a two-fold backflow operator $B^{(2)}_{\langle t_1, t_2, t_3, t_4 \rangle}$ behaves in a limit in which the two backflow intervals merge together, i.e. $t_2, t_3 \to \tau$ for some $\tau \in (t_1, t_4)$, with t_1, t_4 held fixed and maintaining $t_2 < t_3$. An obvious question is whether the spectrum converges in some sense to that of $B^{(1)}_{\langle t_1, t_4 \rangle}$. As we now show, this is not the case. Writing $\text{srsd}\langle t_1, t_2, t_3, t_4 \rangle = (v, w)$, we have $v \to 0+$ and $w \to +\infty$ in the limit. Using the $M = j = k = 1$ case of theorem 4.1, we find

$$\limsup b^{(2)}_{\text{over}}(v, w) \leq -1 - b^{(1)}_{\text{back}} = -1 - c_{\text{BM}}, \tag{4.7}$$

from equation (4.2) in the limit of interest. Hence $b^{(2)}_{\text{over}}(v, w) \to -1 - c_{\text{BM}}$ because we also have $b^{(2)}_{\text{over}} \geq c^{(2)}_{\text{over}} = -1 - c_{\text{BM}}$. Thus, $\sigma(B^{(2)}_{\langle t_1, t_2, t_3, t_4 \rangle})$ contains points approaching $-1 - c_{\text{BM}}$ arbitrarily closely in the limit, while $\sigma(B^{(1)}_{\langle t_1, t_2 \rangle}) \subseteq [-1, c_{\text{BM}}]$. Therefore the spectra do not coincide in the limit; in fact, we have

$$\liminf_{\substack{t_2, t_3 \to \tau \\ t_2 < t_3}} d_{\text{Haus}}(\sigma(B^{(2)}_{\langle t_1, t_2, t_3, t_4 \rangle}), \sigma(B^{(1)}_{\langle t_1, t_4 \rangle})) \geq c_{\text{BM}}, \tag{4.8}$$

where the Hausdorff distance between compact $A, B \subset \mathbb{R}$ is

$$d_{\text{Haus}}(A, B) = \max\{\sup_{a \in A} \inf_{b \in B} |a - b|, \sup_{b \in B} \inf_{a \in A} |a - b|\}, \tag{4.9}$$

and gives the collection of non-empty compact subsets of $\mathbb{R}$ the structure of a complete metric space (e.g. theorem 3.2.4 of [24]). As one has the inequality $d_{\text{Haus}}(\sigma(A), \sigma(B)) \leq ||A - B||$ for self-adjoint bounded operators on Hilbert spaces (e.g. theorem V.4.10 in [25]), we may infer that the

backflow operators $B^{(2)}_{\langle t_1,t_2,t_3,t_4\rangle}$ do not converge in norm to $B^{(1)}_{\langle t_1,t_4\rangle}$ in the limit considered. This can also be seen directly as follows, noting that

$$B^{(2)}_{\langle t_1,t_2,t_3,t_4\rangle} - B^{(1)}_{\langle t_1,t_4\rangle} = -B^{(1)}_{\langle t_2,t_3\rangle} \tag{4.10}$$

and therefore

$$||B^{(2)}_{\langle t_1,t_2,t_3,t_4\rangle} - B^{(1)}_{\langle t_1,t_4\rangle}|| = 1, \tag{4.11}$$

by recalling that all single backflow operators have unit norm. It would be interesting to study other mergers of multiple backflow intervals in a similar way.

We end this discussion with a cautionary note. For $\Lambda > 0$, let $L^2([0,\Lambda],dk)$ be the space of positive-momentum states with momentum cutoff Λ, in momentum representation. Let $\iota_\Lambda : L^2([0,\Lambda],dk) \to L^2(\mathbb{R}^+,dk)$ be the subspace inclusion map, whereupon ι_Λ^* is the subspace projection. Lemma A1 in the electronic supplementary material, §A, shows that the operators $\iota_\Lambda^* B^{(1)}_{\langle s,t\rangle}\iota_\Lambda$ are norm continuous in $\langle s,t\rangle \in \mathcal{T}_2$ with respect to the operator norm $||\cdot||_\Lambda$ on $L^2([0,\Lambda],dk)$. Considering equation (4.10) again, it follows that

$$||\iota_\Lambda^*(B^{(2)}_{\langle t_1,t_2,t_3,t_4\rangle} - B^{(1)}_{\langle t_1,t_4\rangle})\iota_\Lambda||_\Lambda \longrightarrow 0 \tag{4.12}$$

as the backflow intervals merge, so

$$\lim_{t_3-t_2\to 0^+} d_{\mathrm{Haus}}(\sigma(\iota_\Lambda^* B^{(2)}_{\langle t_1,t_2,t_3,t_4\rangle}\iota_\Lambda), \sigma(\iota_\Lambda^* B^{(1)}_{\langle t_1,t_4\rangle}\iota_\Lambda)) \longrightarrow 0 \tag{4.13}$$

in this limit. Accordingly, any numerical scheme implementing a fixed momentum cutoff will give the erroneous impression of a convergence of spectra as backflow intervals merge. To see the true behaviour of the backflow operators as in equation (4.8), it would therefore be necessary to increase the momentum cutoff as $t_3 - t_2$ decreases.

5. Numerical calculation

The goal of this section is to numerically investigate the multiple QB and quantum overflow effect over M disjoint intervals of equal duration separated by gaps of the same length, corresponding to the bounded operator $C^{(M)}$ given in equation (3.14). Although our method would in principle apply to arbitrary M, the computational effort rises quickly with M and we have chosen to restrict to $M \leq 4$. The numerical results give lower bounds on the magnitudes of $b^{(M)}_{\mathrm{back/over}}(1,\ldots,1)$ for $1 \leq M \leq 4$. In particular, we find for $2 \leq M \leq 4$ that $\max\sigma(C^{(M)}) > c_{\mathrm{BM}}$ and $\min\sigma(C^{(M)}) < -1$. This complements the analytic results in theorem 3.2 and corollary 3.3 on the large M asymptotics of $\sigma(C^{(M)})$, and the mononotonicity results in theorem 4.1. By numerical acceleration methods, we shall give improved estimates for $b^{(M)}_{\mathrm{back/over}}(1,\ldots,1)$ for $1 \leq M \leq 4$. In addition, we investigate the properties of states that come close to maximizing the backflow or overflow for these operators.

(a) Background theory

Our numerical calculations are based on the following basic observation. (See §XIII.1 of [26] for a discussion of other min–max results and theorem VII.12 of [27] for Weyl's criterion.) Here, $\sigma(B,Q) = \{\lambda \in \mathbb{R} : \det(B - \lambda Q) = 0\}$ is the set of generalized eigenvalues for Hermitian matrix B with respect to a positive definite matrix Q of the same dimension.

Proposition 5.1. *Let A be a bounded self-adjoint operator on Hilbert space $\mathcal{H}$ and let $(\chi_n)_{n\in\mathbb{N}} \subset \mathcal{H}$ be a sequence of linearly independent vectors with dense span. Define sequences of self-adjoint $N \times N$ matrices*

$(A^{[N]})_{N\in\mathbb{N}}$ and $(P^{[N]})_{N\in\mathbb{N}}$ with matrix elements

$$A^{[N]}_{mn} = \langle \chi_m | A \chi_n \rangle \quad \text{and} \quad P^{[N]}_{mn} = \langle \chi_m | \chi_n \rangle, \tag{5.1}$$

for $1 \le m, n \le N$. Then $\sigma(A^{[N]}, P^{[N]}) \subseteq \mathcal{N}(A)$, and $\max \sigma(A^{[N]}, P^{[N]})$ (resp., $\min \sigma(A^{[N]}, P^{[N]})$) is a bounded non-decreasing (resp., non-increasing) sequence with

$$\max \sigma(A) = \lim_{N\to\infty} \max \sigma(A^{[N]}, P^{[N]}) \quad \text{and} \quad \min \sigma(A) = \lim_{N\to\infty} \min \sigma(A^{[N]}, P^{[N]}). \tag{5.2}$$

For each $N \in \mathbb{N}$, suppose $v^{(N)} \in \mathbb{C}^N$ is a generalized eigenvector obeying

$$A^{[N]} v^{(N)} = \lambda_N P^{[N]} v^{(N)} \quad \text{and} \quad v^{(N)\dagger} P^{[N]} v^{(N)} = 1, \tag{5.3}$$

and define $\psi^{(N)} \in \mathcal{H}$ by

$$\psi^{(N)} = \sum_{n=1}^{N} v^{(N)}_n \chi_n. \tag{5.4}$$

If $\psi^{(N)} \to \psi \in \mathcal{H}$ in norm then

(i) the sequence of generalized eigenvalues $(\lambda_N)_{N\in\mathbb{N}}$ converges;
(ii) the sequence of vectors $(\psi^{(N)})_{N\in\mathbb{N}}$ is a Weyl sequence for $\lambda = \lim_{N\to\infty} \lambda_N$, i.e. $||\psi^{(N)}|| = 1$ and $||(A - \lambda I)\psi^{(N)}|| \to 0$;
(iii) the limiting vector ψ is an eigenvector for A with eigenvalue λ.

The proof of proposition 5.1 may be found in the electronic supplementary material, §E. The generalized eigenvalue problems in proposition 5.1 reduce to standard eigenvalue problems if the trial vectors χ_n are orthonormal. In principle one could always orthogonalize to express the matrix elements in a Gram–Schmidt basis, but this introduces a non-trivial computational overhead and the generalized eigenproblem may be preferred.

(b) Numerical methodology and results

We apply proposition 5.1 to the operators $C^{(M)}$, but our methodology also applies to general backflow operators. Given $\delta > -1/2$ and $a > 0$, define the sequence of normalized $L^2(\mathbb{R}^+, dq)$ vectors $(\psi_{n,a,\delta})_{n=0}^{\infty}$ by

$$\psi_{n,a,\delta}(q) = E_n(a,\delta) q^{n+\delta} e^{-aq}, \tag{5.5}$$

with the normalization constant $E_n(a,\delta)$ given by

$$E_n(a,\delta) = \frac{(2a)^{n+\delta+1/2}}{\sqrt{\Gamma(2n+2\delta+1)}}. \tag{5.6}$$

The following density result is found in theorem 5.7.1 of [28] in the case $a = 1/2$, and follows for general $a > 0$ followed by a unitary scale change.

Lemma 5.2. *For $a > 0$ and $-\frac{1}{2} < \delta < \frac{1}{2}$, the sequence $(\psi_{n,a,\delta})_{n=0}^{\infty}$ has a dense span in $L^2(\mathbb{R}^+, dq)$.*

To apply proposition 5.1 to $C^{(M)}$, we require the matrix elements

$$C^{(M)}(a,\delta)_{mn} = \langle \psi_{m,a,\delta} | C^{(M)} \psi_{n,a,\delta} \rangle \quad \text{and} \quad P(a,\delta)_{mn} = \langle \psi_{m,a,\delta} | \psi_{n,a,\delta} \rangle, \tag{5.7}$$

for $m, n \in \mathbb{N}_0$. The components $P(a,\delta)_{mn}$ admit the closed form

$$P(a,\delta)_{mn} = \frac{\sqrt{B_{\mathrm{diag}}(m+\delta+1/2) B_{\mathrm{diag}}(n+\delta+1/2)}}{B(m+\delta+1/2, n+\delta+1/2)}, \tag{5.8}$$

where $B(x,y) = \Gamma(x)\Gamma(y)/\Gamma(x+y)$ is the beta function and $B_{\mathrm{diag}}(x) = B(x,x) = \Gamma(x)^2/\Gamma(2x)$. The components $C^{(M)}(a,\delta)_{mn}$ (or indeed, those of general multiple backflow operators) also have a

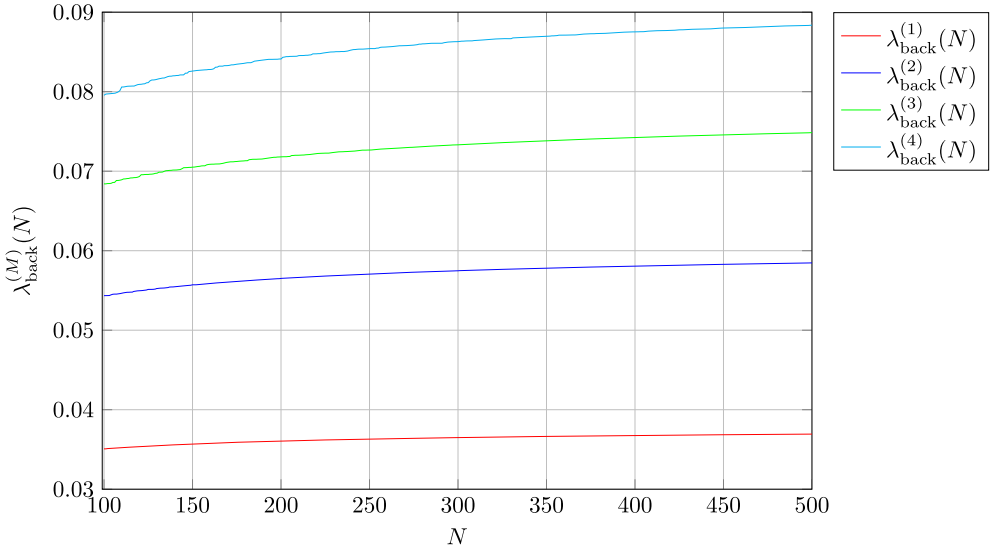

Figure 4. Plot of $\lambda^{(M)}_{\text{back}}(N)$ for $100 \leq N \leq 500$.

closed form expression in terms of incomplete beta functions, for which the reader is referred to electronic supplementary material, §F. For each M, and for fixed $a > 0$, $\delta \in (-1/2, 1/2)$, the matrix elements $P(a,\delta)_{mn}$ and $C^{(M)}(a,\delta)_{mn}$ can be computed for $0 \leq m, n \leq N$, giving $(N+1)$-dimensional square matrices. The matrix elements must be computed to high precision, for which purpose we use the package FLINT [17,18]. For a discussion of the error analysis of the generalized eigenvalues, the reader is guided to electronic supplementary material, §G.

Further experimentation was used to find the values of a_M, δ_M that appear to produce the best, i.e. approximately largest magnitude, values of $\lambda^{(M)}_{\text{back/over}}(a,\delta;N)$ for given M across the range of N studied, resulting in choices $a_M = 2M/\pi$ and $\delta_M = -1/4$. (We do not claim that these values are precisely optimal.) Our choice relies on the following observations. Each $\psi_{n,a,\delta}(q)$ has a unique global maximum at $q = a^{-1}(n+\delta)$ and hence for each number of backflow periods M, we expect that a good choice of a_M^{-1} would be comparable with the gap between consecutive peaks of the top approximate eigenvector $\psi^{(M)}_{\text{back}}(a,\delta;N)$. Early numerical results suggested that for $M = 1$, this gap tends to π as N increases and the best numerical results were found when using $a_1 = 2/\pi$. For larger values of M, the top approximate eigenvector has M times as many stationary points (see figures 8, 10 and 12 below) and so we selected $a_M = Ma_1 = 2M/\pi$. To motivate the choice $\delta_M = -1/4$, consider the action of a vector of the form $\psi(q) = q^{-1/4}f(q)$ under $C^{(M)}$, we find

$$(C^{(M)}\psi)(p) = -\frac{p^{-1/4}}{4\pi}\int_0^\infty \mathrm{d}q \frac{\sin(2M(p-q))}{(p-q)\cos(p-q)} f(q) - \frac{p^{1/4}}{4\pi}\int_0^\infty \mathrm{d}q \frac{\sin(2M(p-q))}{(p-q)\cos(p-q)} q^{-1/2} f(q), \tag{5.9}$$

suggesting that any eigenfunction of $C^{(M)}$ is likely to diverge as $\mathcal{O}(p^{-1/4})$ as $p \to 0^+$. We define $\lambda^{(M)}_{\text{back/over}}(N) = \lambda^{(M)}_{\text{back/over}}(a_M, -\frac{1}{4}; N)$.

We present numerical results for $M \in \{1,2,3,4\}$ in graphical form in figures 4 and 5 for $100 \leq N \leq 500$ and list the values of $\lambda^{(M)}_{\text{back/over}}(500)$ in table 1. The values obtained for all N stored at 150 digits may be found in the research data repository of the University of York [29]. Note that the N^{th} eigenvalue should only be trusted to approximately $503 - 0.91N$ decimal places. The plots display the values for $N \geq 100$, over which range they increasingly resemble smooth curves. Each separate eigenvalue sequence is monotonic and would tend to the maximum or minimum of the appropriate spectrum $\sigma(C^{(M)})$ as $N \to \infty$. We discuss the convergence rates and estimated limits with more detail in the next subsection, but it is already clear that the $M = 1$

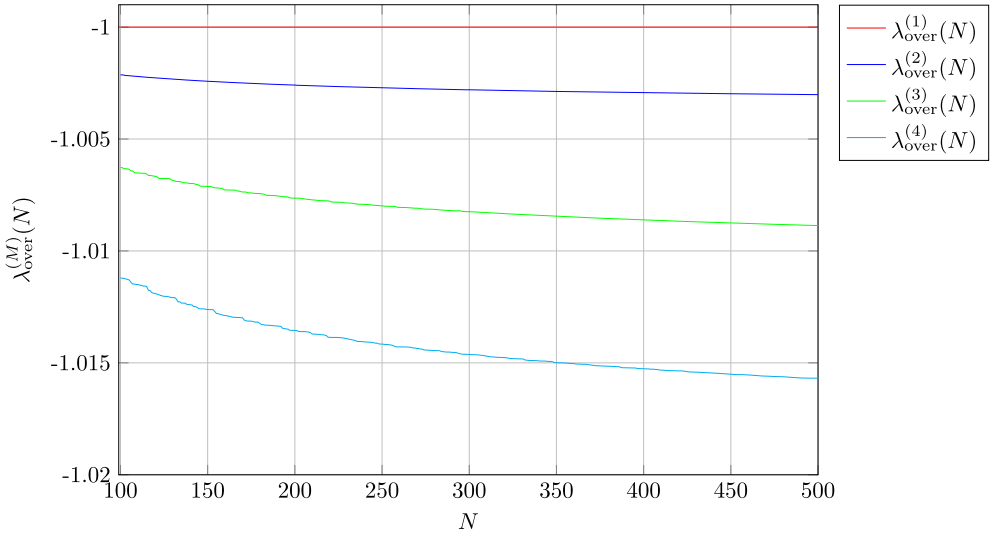

Figure 5. Plot of $\lambda^{(M)}_{\text{over}}$ for $100 \leq N \leq 500$.

Table 1. Values of $\lambda^{(M)}_{\text{back/over}}(500)$ and $d^{(M)}_{\text{back}}(499, 500)$ for $1 \leq M \leq 4$.

M	$\lambda^{(M)}_{\text{back}}(500)$	$\lambda^{(M)}_{\text{over}}(500)$	$d^{(M)}_{\text{back}}(499, 500)$
1	0.036933	−1	0.0058
2	0.058464	−1.0030	0.0017
3	0.074860	−1.0089	0.0041
4	0.088378	−1.0157	0.0084

values stay below the previously estimated value of the Bracken–Melloy constant $c_{\text{BM}} \approx 0.03845$ [3,16], that one has $c^{(M)}_{\text{back}} \geq b^{(M)}_{\text{back}}(1, \ldots, 1) > c_{\text{BM}}$ and $c^{(M)}_{\text{over}} \leq b^{(M)}_{\text{over}}(1, \ldots, 1) < -1$ for $2 \leq M \leq 4$, and that the value of $b^{(2)}_{\text{over}}(1, 1)$ appears to be much closer to -1 than to the 2-fold overflow constant $c^{(2)}_{\text{over}} = -1 - c_{\text{BM}}$.

As well as estimates for the backflow and overflow values of $C^{(M)}$, we also computed the associated approximate eigenvectors as follows. As in proposition 5.1, each vector $v \in \mathbb{R}^{N+1}$ with $v^{\dagger} P^{[N]}(a, \delta) v = 1$ defines an approximate eigenvector $\psi \in L^2(\mathbb{R}^+)$ for $C^{(M)}$,

$$\psi = \sum_{n=0}^{N} v_n \psi_n(a, \delta; \cdot). \tag{5.10}$$

Define $\psi^{(M)}_{\text{back/over}}(a, \delta; N; \cdot)$ as the $L^2(\mathbb{R}^+)$ vector given by applying equation (5.10) to the generalized eigenvectors associated with the largest/smallest generalized eigenvalues of $(C^{(M)[N]}(a, \delta), P^{[N]}(a, \delta))$. Figure 6 shows the vectors $\psi^{(M)}_{\text{back}}(a_M, -1/4; 500; p)$ for $p \in [0, 10]$. As can be seen, all the M-fold backflow maximizing vectors appear to diverge as $p \to 0$. In line with $\delta = -1/4$ giving the best approximate eigenvalue results, we conjecture that all of the M-fold backflow maximizing vectors behave like $p^{-1/4}$ for $p \sim 0$. Recall from §3b that the momentum space wavefunction is obtained by applying the unitary $U^* : L^2(\mathbb{R}^+, dp) \to L^2(\mathbb{R}^+, dk)$ implementing a change of variables $p = k^2/2$, where we set the unit of time equal to the duration and spacing of the backflow intervals and use units of mass and length so that $m = 1/2$ and $\hbar = 1$. As $(U^* \psi)(k) = \sqrt{k} \psi(k^2/2)$, our conjecture is that the momentum wavefunctions of M-fold backflow maximizing vectors have finite limits as $k \to 0+$.

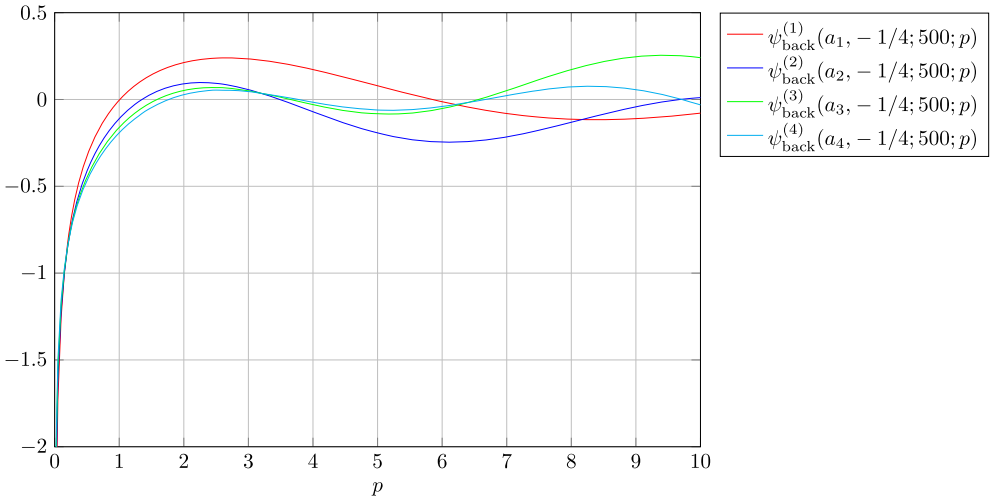

Figure 6. Plot of $\psi^{(M)}_{\text{back}}(a_M, -1/4; 500; p)$ for $p \in [0, 10]$

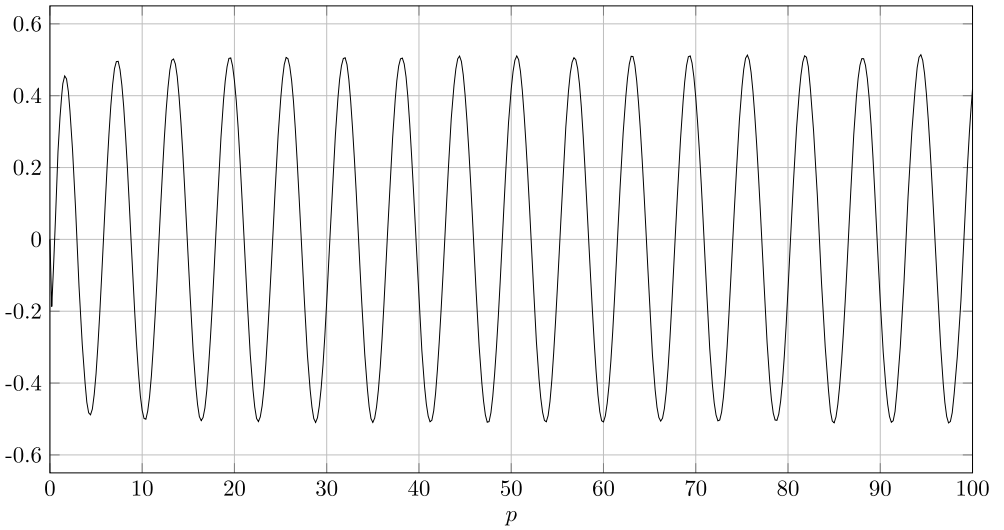

Figure 7. Plot of $p^{3/4}\psi^{(1)}_{\text{back}}(a_1, -1/4; 500; p)$ for $p \in [0, 100]$

Figures 7–14 show the approximate backflow and overflow eigenvectors for $1 \leq M \leq 4$ as functions of p. A common feature is that the envelope of the wavefunction decays as $p^{-3/4}$ for large p; in all cases except for $\psi^{(1)}_{\text{over}}(a_1, -1/4; 500); p)$, we plot the eigenfunction multiplied by a factor of $p^{3/4}$ to better illustrate the oscillatory structure. From figures 8, 10 and 12, one sees that all $M \geq 2$ backflow vectors have higher frequency contributions when compared with the $M = 1$ backflow vector. This is not a surprise when considering the integral kernel of the $C^{(M)}$ for $M \geq 2$ in equation (3.14).

At time t, the position wavefunction of a state with time-zero momentum wavefunction $\phi(k)$ is

$$(\mathcal{R}_t\phi)(x) = \frac{1}{\sqrt{2\pi}} \int_0^\infty \mathrm{d}k\, \mathrm{e}^{\mathrm{i}xk - ik^2 t}\phi(k). \tag{5.11}$$

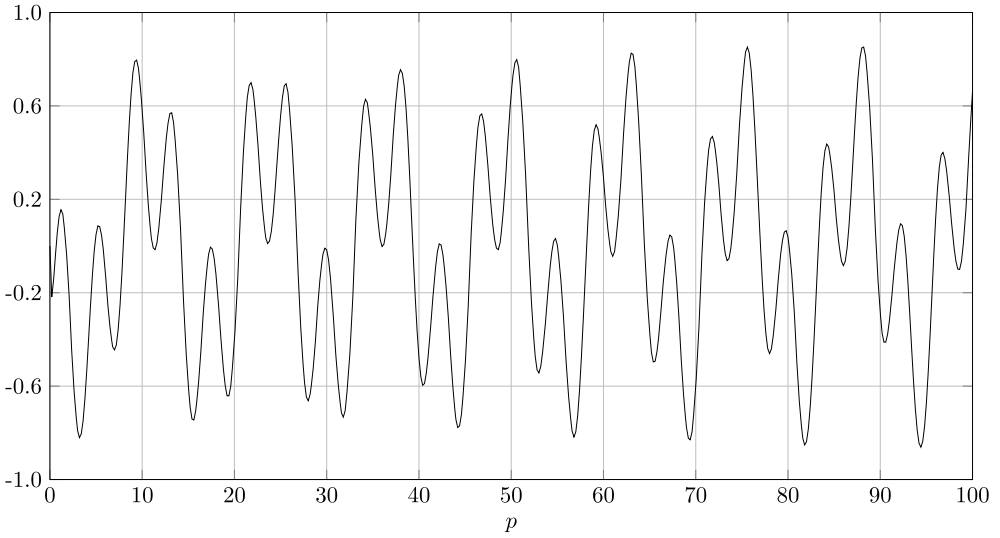

Figure 8. Plot of $p^{3/4}\psi^{(2)}_{\text{back}}(a_2, -1/4; 500; p)$ for $p \in [0, 100]$

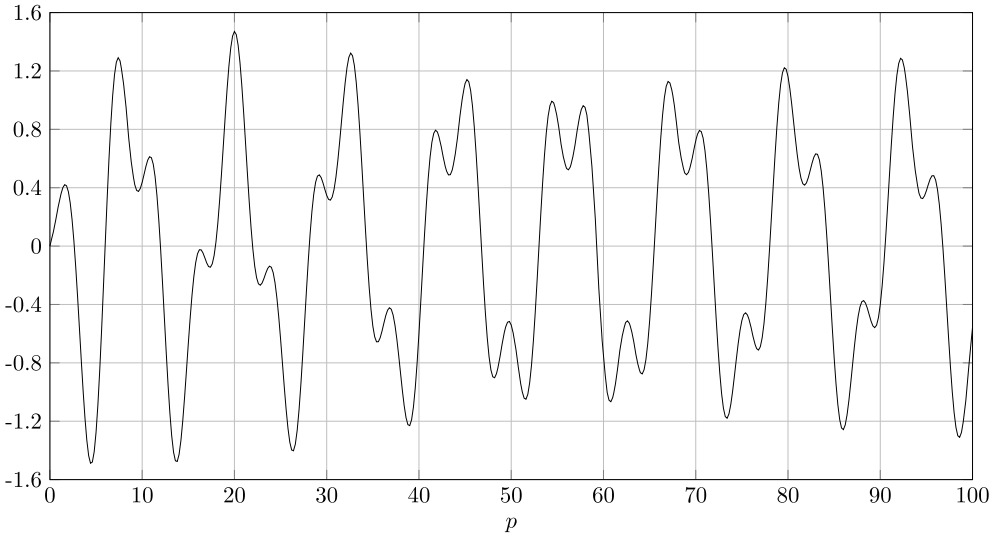

Figure 9. Plot of $p^{3/4}\psi^{(2)}_{\text{over}}(a_2, -1/4; 500; p)$ for $p \in [0, 100]$

Using a special function representation of $\mathcal{R}_t U^* \psi_{m,a,\delta}$, the time evolved position probability densities were computed for backflow/overflow-maximizing states with time-zero position wavefunctions:

$$\chi^{(M)}_{\text{back/over}} = \mathcal{R}_0 U^* \psi^{(M)}_{\text{back/over}}(a_M, 1/4; 100; \cdot). \tag{5.12}$$

Here, $N = 100$ was used to reduce computational overheads. The corresponding time-zero position probability densities are plotted in figures 15, 16 and 17, while the time-evolved probability densities appear in figures 2 and 3 for $M = 2$, and the probability fluxes of $\chi^{(M)}_{\text{back}}$ at $x = 0$ are shown in figure 1. Further plots may be found in the electronic supplementary material, §J.

As shown in proposition 5.1, if the sequences $(\psi^{(M)}_{\text{back/over}}(a_M, -1/4; N; \cdot))_{N\in\mathbb{N}}$ converge in norm, then they are Weyl sequences and the associated limiting vector and spectral point constitute an

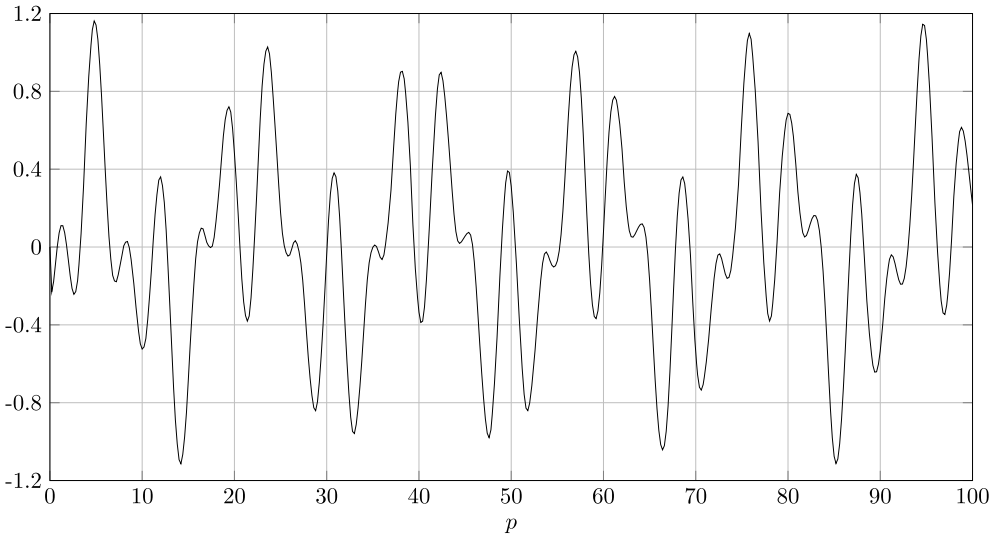

Figure 10. Plot of $p^{3/4}\psi^{(3)}_{\text{back}}(a_3, -1/4; 500; p)$ for $p \in [0, 100]$

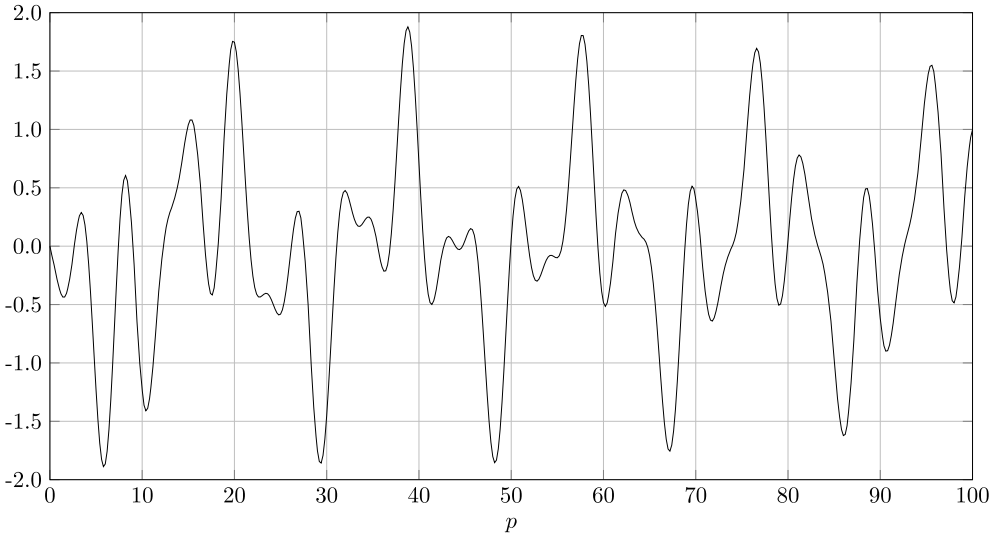

Figure 11. Plot of $p^{3/4}\psi^{(3)}_{\text{over}}(a_3, -1/4; 500; p)$ for $p \in [0, 100]$

eigenpair. For integers n, m, let $d^{(M)}_{\text{back/over}}(n, m)$ be defined as

$$d^{(M)}_{\text{back/over}}(n, m) = ||\psi^{(M)}_{\text{back/over}}(a_M, -1/4; n; \cdot) - \psi^{(M)}_{\text{back/over}}(a_M, -1/4; m; \cdot)||_{L^2(\mathbb{R}^+)}. \tag{5.13}$$

As a crude test, we have computed $d^{(M)}_{\text{back}}(N, 500)$ for $1 \le N \le 499$. For each $M = 1, 2, 3, 4$ the values form a decaying non-increasing sequence with final values listed in table 1 alongside the final value for each of the sequences $\lambda^{(M)}_{\text{back/over}}$.

Similar results are obtained for the norm differences of overflow vectors $d^{(M)}_{\text{over}}(N, 500)$ for $1 \le N \le 499$ and $M = 2, 3, 4$. Though far from a rigorous proof, our numerical results suggest

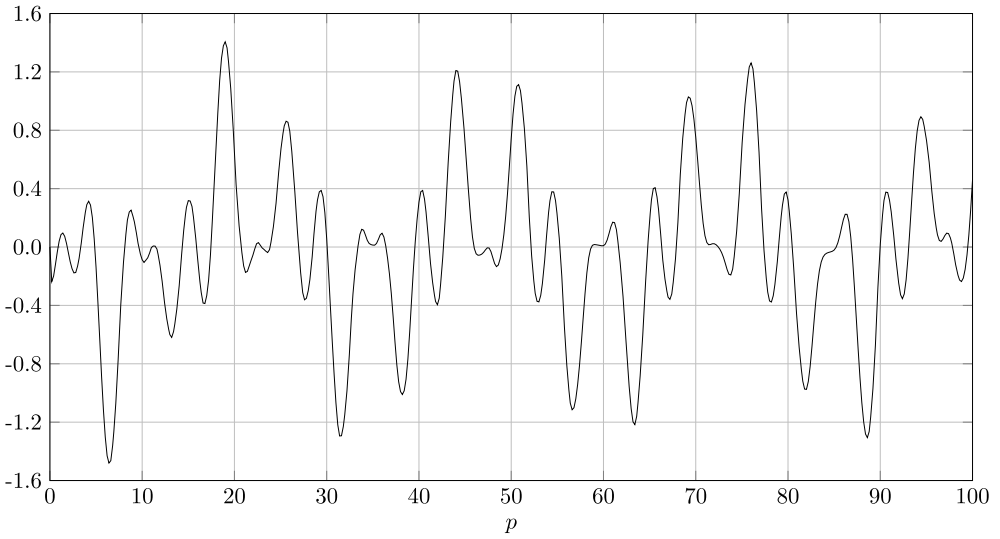

Figure 12. Plot of $p^{3/4}\psi^{(4)}_{\text{back}}(a_4, -1/4; 500; p)$ for $p \in [0, 100]$

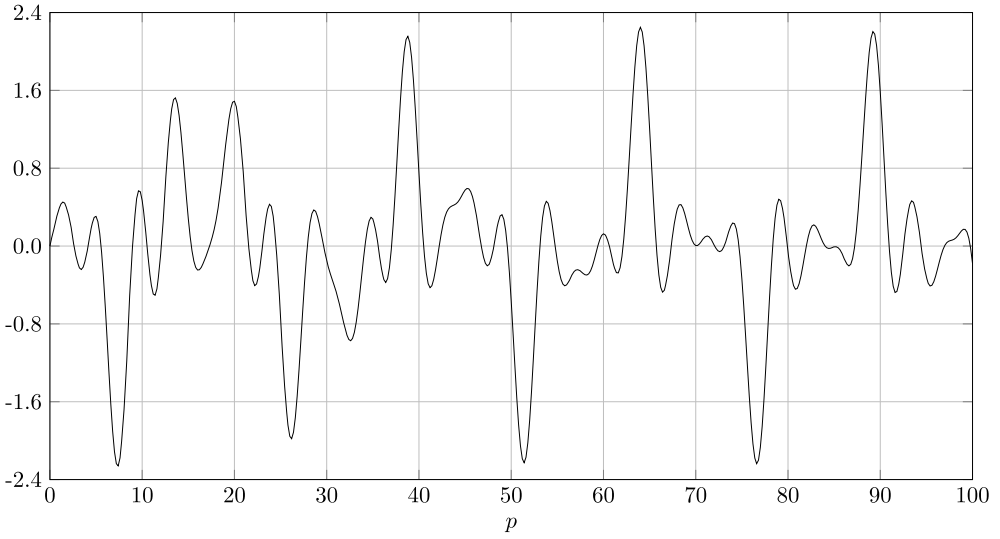

Figure 13. Plot of $p^{3/4}\psi^{(4)}_{\text{over}}(a_4, -1/4; 500; p)$ for $p \in [0, 100]$

that $b^{(M)}_{\text{back}}(1, \ldots, 1) = \max \sigma(C^{(M)})$ is an eigenvalue of $C^{(M)}$ for $1 \leq M \leq 4$, while $b^{(M)}_{\text{over}}(1, \ldots, 1) = \min \sigma(C^{(M)})$ is an eigenvalue of $C^{(M)}$ for $2 \leq M \leq 4$.

The infimum of the spectrum of the $M = 1$ operator $C^{(1)}$ requires particular discussion. Figure 14 shows the vectors $\psi^{(1)}_{\text{over}}(a_1, -1/4; N)$ for N running from 50 to 450 inclusive in multiples of 50, generated from $N_{\max} = 500$ data. Each plot consists of a single peak centred approximately at $1.5N$, which broadens as N increases. This suggests a sequence of vectors weakly converging to the zero vector in $L^2(\mathbb{R}^+, dp)$ as N increases, whose $C^{(1)}$-expectation values tend to -1. Such a sequence would constitute a singular Weyl sequence for $C^{(1)}$ at -1, from which one could deduce that $-1 \in \sigma_{\text{ess}}(C^{(1)})$ (e.g. theorem 2 in of [30]) – a fact that was proved rigorously in [4]. Our numerical results are therefore in line with this result.

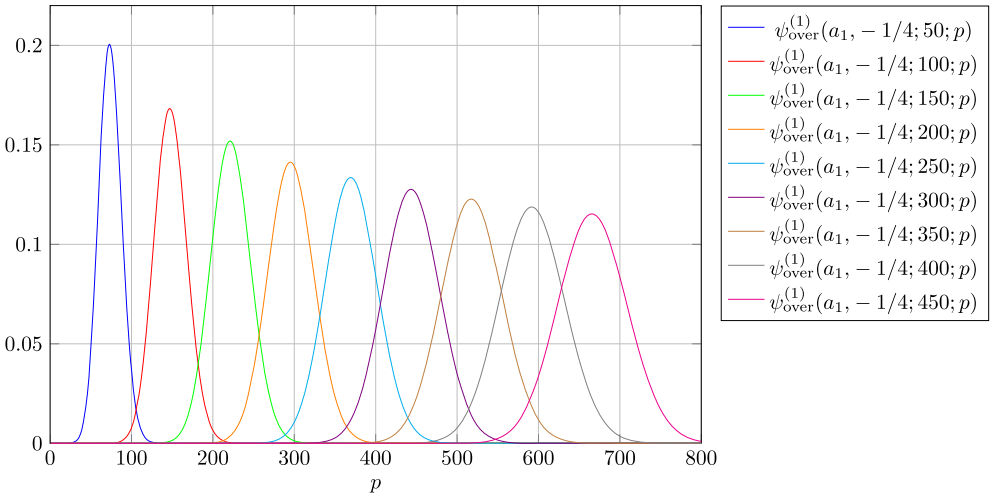

Figure 14. Plots of $\psi^{(1)}_{\text{over}}(a_1, -1/4; N; p)$ for N in multiples of 50 and $p \in [0, 800]$.

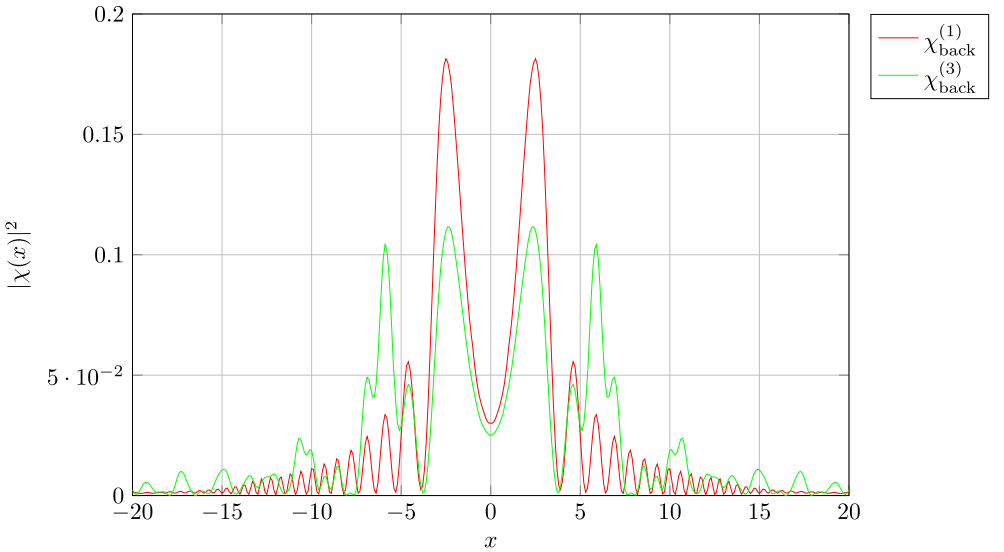

Figure 15. Position probability distribution of the $M = 1, 3$ backflow states $\chi^{(M)}_{\text{back}}$ at time $t = 0$.

(c) Numerical acceleration

The sequences $\lambda^{(M)}_{\text{back/over}}$ are guaranteed to converge to the backflow/overflow values $b^{(M)}_{\text{back/over}}(1, \ldots, 1)$, but the rate of convergence is slow. For example, $\lambda^{(1)}_{\text{back}}(500) = 0.03693$ can be compared with the expected value $b^{(1)}_{\text{back}} = 0.03845$ to four significant figures. In this section we consider numerical acceleration techniques that modify a convergent sequence, while preserving its limit, but increasing the speed of convergence, at least for sequences of interest. The aim is to provide a better estimate of the eventual limit from the available data. This is done with using sequence acceleration.

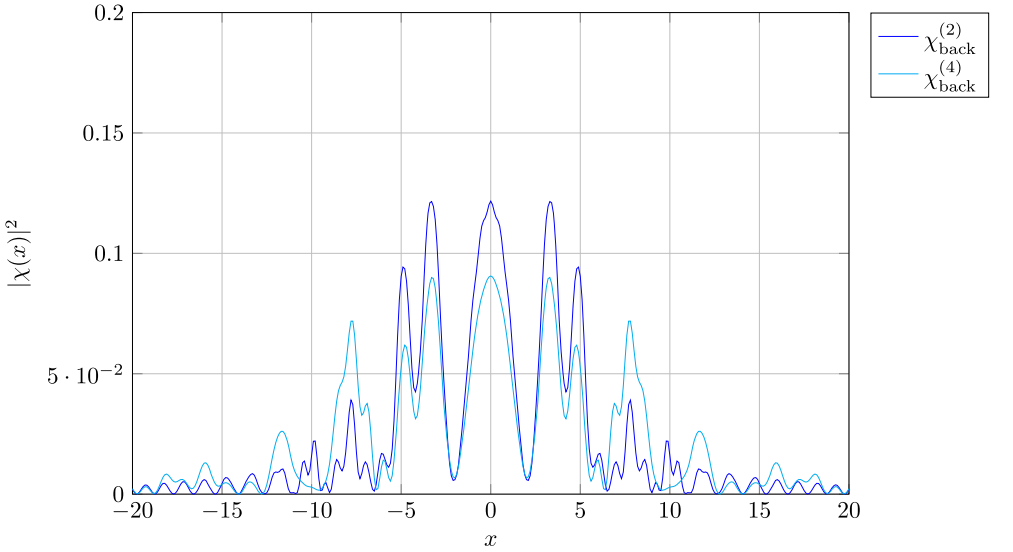

Figure 16. Position probability distribution of the $M = 2, 4$ backflow states $\chi^{(M)}_{\text{back}}$ at time $t = 0$.

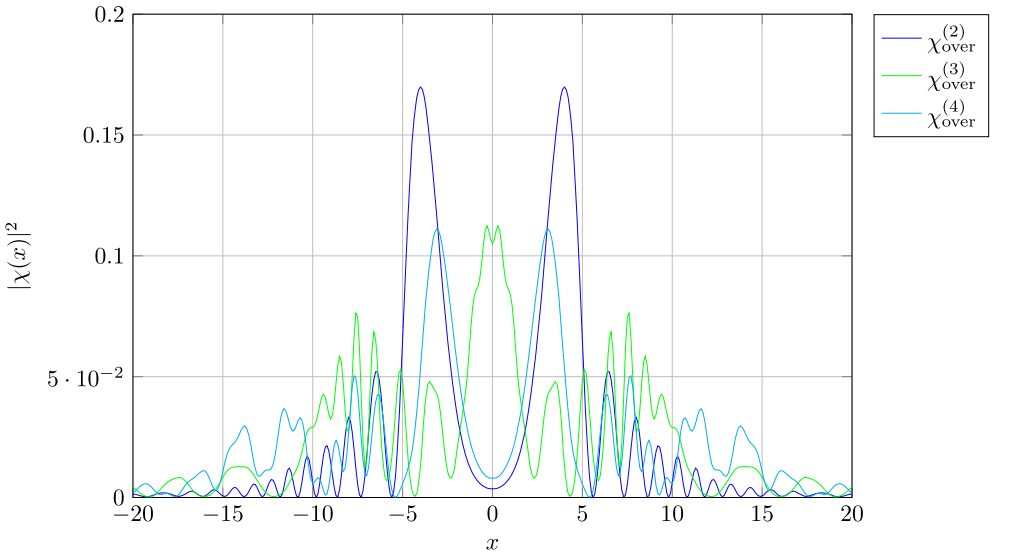

Figure 17. Position probability distribution of the $M = 2, 3, 4$ overflow states $\chi^{(M)}_{\text{over}}$ at time $t = 0$.

Our aim is to apply (generalized) Richardson accelerators, detailed in the electronic supplementary material, §H, to the sequences $\lambda^{(M)}_{\text{back/over}}$ for $1 \leq M \leq 4$. Briefly, suppose that a sequence $(x_n)_{n\in\mathbb{N}}$ has asymptotic form

$$x_n = \sum_{j=1}^{k} \frac{a_j}{n^{\gamma_j}} + \epsilon_n \quad \text{and} \quad |\epsilon_n| \leq \frac{C}{n^{\gamma_{k+1}}}, \tag{5.14}$$

where $0 = \gamma_1 < \gamma_2 < \cdots < \gamma_k < \gamma_{k+1}$, and $a_1, \ldots, a_k$ and C are constant real numbers, so $x_n \to a_1$ as $n \to \infty$. Writing $\boldsymbol{\gamma} = (\gamma_1, \ldots, \gamma_{k+1})$, the generalized Richardson accelerator $R_{\boldsymbol{\gamma}}$ is a linear map on

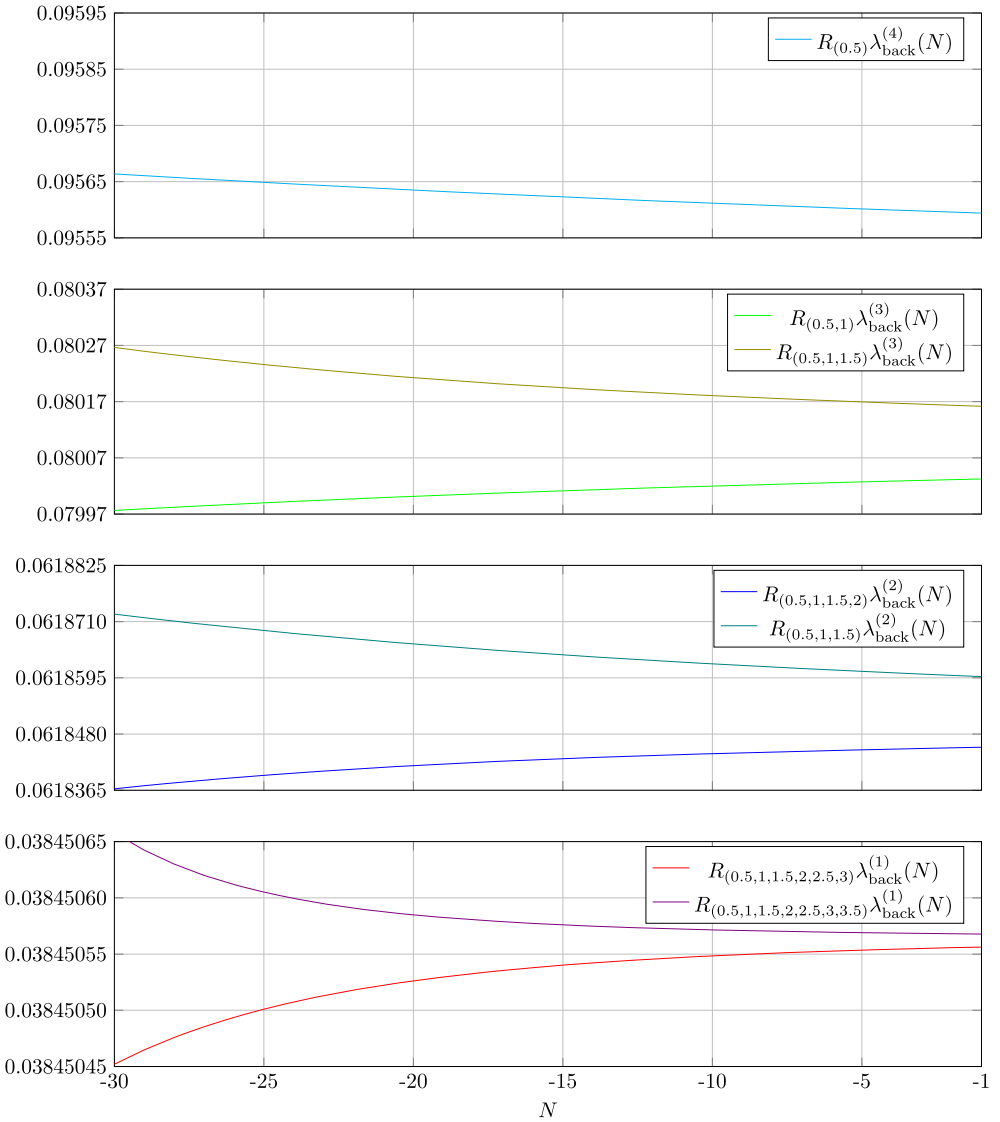

Figure 18. Plots of $R_{\boldsymbol{\gamma}_M}\lambda^{(M)}_{\text{back}}$ for selected powers $\boldsymbol{\gamma}_M$ and $1 \leq M \leq 4$.

sequences with the property that

$$(R_{\boldsymbol{\gamma}}x)_n = a_1 + (R_{\boldsymbol{\gamma}}\epsilon)_n \quad \text{and} \quad |(R_{\boldsymbol{\gamma}}\epsilon)_n| \leq \frac{C_{\boldsymbol{\gamma}}}{n^{\gamma_{k+1}}}, \tag{5.15}$$

where the constant $C_{\boldsymbol{\gamma}}$ can be computed explicitly. Thus the rate of convergence is improved.

As the asymptotics of the sequences $\lambda^{(M)}_{\text{back/over}}$ are unknown we performed tests that suggest strongly that they have an asymptotic form like the above with half-integer exponents. Another issue is that the sequences $\lambda^{(M)}_{\text{back}}$ contain oscillatory components with amplitude and period increasing with M. These oscillations become apparent in the accelerated sequences, once the dominant power law terms are removed, obstructing attempts to estimate the limit. Details of the oscillatory damping and evidence for the ansatz can be found in the electronic supplementary material, §I.

Table 2. Conjectured upper and lower bounds for c_{BM} and $b^{(M)}_{\mathrm{back}}(1,\ldots,1)$ for $1 \le M \le 4$.

M	acceleration parameters	lower bound (LB)	upper bound (UB)
1	LB: (0.5, 1, 1.5, 2, 2.5, 3), UB: (0.5, 1, 1.5, 2, 2.5, 3, 3.5)	0.0384505563	0.0384505678
2	LB: (0.5, 1, 1.5, 2), UB: (0.5, 1, 1.5)	0.0618453024	0.0618597497
3	LB: (0.5, 1), UB: (0.5, 1, 1.5)	0.0800324618	0.0801617473
4	UB: (0.5)	—	0.0955940854

Using generalized Richardson accelerators, we obtain conjectural bounds on c_{BM}. Application of $R_{(0.5,1,1.5,2,2.5,3)}$ and $R_{(0.5,1,1.5,2,2.5,3,3.5)}$ to $\lambda^{(1)}_{\mathrm{back}}$ result in descending and ascending sequences, respectively, as shown in figure 18. By selecting the final values of each sequence, we obtain conjectured upper and lower bounds to the Bracken–Melloy constant. To eight significant figures, we find

$$0.038450556 \le c_{\mathrm{BM}} \le 0.038450568 \tag{5.16}$$

and thus $c_{\mathrm{BM}} = 0.0384506$ correct to the first six significant figures. Of particular note is that the upper bound we obtain is strictly below the previously accepted figure of 0.038452. Possible reasons for this are discussed below. Note that while the accelerators we use result in sequences whose eventual limit is guaranteed to be equal to c_{BM}, it is conceivable that the limited number of terms available may give a misleading impression. For example, we cannot be sure that the two sequences arising from $R_{(0.5,1,1.5,2,2.5,3)}$ and $R_{(0.5,1,1.5,2,2.5,3,3.5)}$ remain monotonic and provide upper and lower bounds to c_{BM}. If more terms were computed, these sequences might cross, perhaps many times, before approaching their common limit. However, problems of this sort are common to all numerical computation that is unsupported by rigorous bounds. We are currently conducting an independent calculation of c_{BM} which it is hoped will serve as a cross-check on these values.

Our estimate for c_{BM} agrees with those of [3,4] to four significant figures but differs beyond that. In fact the fifth significant figure in [3] was stated tentatively, though it was then apparently confirmed and refined in [4]. We briefly compare the methods used to argue that our new estimate is likely to be the more accurate of the three, based on the following two observations. First, in [3,4] the backflow operator (or an operator unitarily equivalent to it) on $L^2(\mathbb{R}^+)$ was numerically diagonalized by truncating to a subspace $L^2([0,\Lambda])$ and then discretizing the resulting operator by setting a mesh size $\delta \ll \Lambda$ resulting in a matrix problem of dimension $\mathcal{O}(\Lambda/\delta)$. Although the techniques in [3,4] were different in detail, they share the feature that c_{BM} is obtained in a double limit $\delta \to 0$ and $\Lambda \to \infty$. In practice, a mesh size $\delta(\Lambda) > 0$ is selected that appears to give reasonable estimate of the $\delta \to 0$ limit at fixed Λ, and a sequence of results is obtained by increasing Λ through some sequence of cutoff sizes Λ_N. Consequently, the sequence of results can depend on the sequence Λ_N as well as the dependence of δ on Λ. By contrast, our method is based on closed form expressions for the matrix elements in terms of special functions, avoiding cutoffs and discretization. Once we have chosen our sequence of basis functions, the sequence of eigenvalue estimates is labelled by the single parameter N that indicates how many basis vectors have been used; we are also able to compute these estimates to high precision based on the error analysis in §5a. Second, [3,4] used relatively straightforward fitting or extrapolation methods to estimate the limiting value c_{BM}, whereas we have used sequence acceleration to systematically remove terms in the asymptotic series resulting in sequences that converge significantly faster to c_{BM} than the raw sequence $\lambda^{(1)}_{\mathrm{back}}$.

Table 3. Conjectured upper and lower bounds of $b^{(M)}_{\text{over}}(1,\ldots,1)$ for $M=2,3,4$ intervals of equal length and spacing.

M	acceleration parameters	lower bound (LB)	upper bound (UB)
2	LB: (0.5, 1, 1.5), UB: (0.5, 1, 1.5, 2)	−1.0037916	−1.0037899
3	LB: (0.5, 1, 1.5), UB: (0.5, 1)	−1.011078	−1.011029
4	UB: (0.5), (0.5, 1)	−1.01947	−1.01934

Plots of the accelerated sequences are presented in figure 18, with the resulting bounds listed in table 2. As with the $M=1$ case, these 'bounds' are not rigorous, but indicate that accelerated sequences appear to sandwich the limiting value.

As a check on our attempts to numerically accelerate $\lambda^{(1)}_{\text{back}}$, we also made use of theorem 5 from [31], which gives a nonlinear acceleration method based on the Raabe–Duhamel (RD) convergence test.

Theorem 5.3. *If a sequence x obeys*

$$\lim_{n\to\infty}\left[(n+1)\frac{x_{n+2}-x_{n+1}}{x_{n+1}-x_n}-n\right]<0, \tag{5.17}$$

then x converges and the nonlinear sequence transformation,

$$\mathrm{RD}[x]_n = x_n - \frac{n(x_{n+1}-x_n)^2}{(n+1)(x_{n+2}-x_{n+1})-n(x_{n+1}-x_n)}, \tag{5.18}$$

accelerates the convergence of x.

The sequence $\lambda^{(1)}_{\text{back}}$ appears to satisfy equation (5.17) for large N, as does $\mathrm{RD}^k[\lambda^{(1)}_{\text{back}}]$ for $k=1,2,3$. After four applications of theorem 5.3 (with some intermediate smoothing to damp oscillations) to $\lambda^{(1)}_{\text{back}}$, we find $c_{\text{BM}}\approx 0.0384506$, backing up the values we find in table 2 from the generalized Richardson accelerator. We were only able to apply the accelerator once to each of the sequences $\lambda^{(M)}_{\text{back}}$ for $M=2,3,4$ and the Richardson results of table 2 appear to be more stable estimates on the basis of the data for $N=500$, though they rely on our assumption that the asymptotic behaviour mirrors that in the $M=1$ case.

We now turn to the analysis of the minimum spectral estimates $\lambda^{(M)}_{\text{over}}$ for $2\le M\le 4$. Note that we do not include any analysis of $M=1$ since it is known that $\lambda^{(1)}_{\text{over}}(N)\to\min\sigma(C^{(1)})=-1$ as $N\to\infty$. Our analysis follows that of the maximum spectral estimates and we assume that each $\lambda^{(M)}_{\text{over}}$ has asymptotics of the same type as $\lambda^{(M)}_{\text{back}}$. We damped oscillations in $\lambda^{(M)}_{\text{over}}$ by the same methodology as before and then applied the generalized Richardson accelerators to accelerate the convergence of the minimum spectral estimates.

The final values of the generalized Richardson accelerated overflow estimates are listed in table 3. The values are written as upper and lower bounds on the overflow values $b^{(M)}_{\text{over}}(1,\ldots,1)$ for M intervals of equal length and spacing, in line with the assumption that the monotonicity of the sequences remain fixed. We note in particular that the overflow value $b^{(2)}_{\text{over}}(1,1)$ for two intervals of equal length and spacing is far from the $M=2$ overflow constant $c^{(2)}_{\text{over}}=-1-c_{\text{BM}}$ arising from all possible pairs of intervals.

6. Conclusion

We have shown that a free particle in one-dimensional quantum mechanics with non-negative momenta can exhibit probability flow in the opposite direction to its momentum over multiple

disjoint time intervals. In particular, given a positive integer M number of time intervals, we have found that the total amount of backflow can grow as $M^{1/4}$.

Similarly, we have shown the total probability flow in the same direction as the particle's momentum can exceed unity. By contrast, we have shown that the total backflow for statistical ensembles of classical particles is bounded within the interval $[-1, 0]$. This result follows a host of phenomena relating quantized observables compared to their classical counterparts. As has been shown, classical observables which have sharp bounds on their values often have quantized counterparts whose values exceed these bounds [3]. The same is true for the case of total probability flow. As already noted, it could be profitable to study overflow without the restriction to positive-momentum states.

Here it is worth making a comment regarding Tsirelson precession, which has already been noted to have a connection with probability backflow in the preprint [32]. Tsirelson showed that if a uniformly precessing coordinate is measured at a randomly chosen angle $\theta \in \{0, 2\pi/3, 4\pi/3\}$, then the probability P that the measured coordinate is positive is bounded for classical systems by $P_{\text{classical}} \leq 2/3$ [33]. However, there exist quantum systems that violate this inequality. In the PhD thesis of Zaw [34], it is shown that for a generalization of the Tsirelson's protocol to an odd number $2M + 1$ of angles, the maximum quantum violation seems to grow like $M^{1/4}$. Further work is being conducted to make the relationship between multiple QB and this generalization of Tsirelson's protocol precise.

We have illustrated our analytical results with numerical calculations of backflow and overflow. In particular this shows that the backflow constants $c^{(M)}_{\text{back}}$ are strictly greater than $c^{(1)} = c_{\text{BM}}$ for $M = 2, 3, 4$, and provides a new estimate of the Bracken–Melloy constant $c_{\text{BM}} \approx 0.0384506$ to six significant figures. This estimate relies on numerical acceleration techniques and appears robust. An independent calculation is in progress and will provide a cross-check.

QB over a single time interval can be attributed to the ability of the quantum mechanical current of a quantum state to attain arbitrarily negative values. The existence of backflow over multiple disjoint time regions indicates that, ignoring effects of measurement on the state, this phenomena can repeat. That is, there exist states ψ with non-negative momentum for which a time of arrival detector would repeatedly detect the the state crossing $x = 0$. Furthermore, the calculation in §3 shows that, as the number M of disjoint time intervals grows, the maximal backflow grows at least as fast as $\mathcal{O}(M^{1/4})$. This larger effect potentially opens a new avenue to experimentally verify QB. However, the fact that this requires measurements of probability differences at many different times presents a challenge that would have to be overcome.

Data accessibility. The data supporting this research are available for download from the research data repository of the University of York [29].

The data are provided in the electronic supplementary material [35].

Declaration of AI use. We have not used AI-assisted technologies in creating this article.

Authors' contributions. C.J.F.: conceptualization, formal analysis, investigation, methodology, supervision, writing—original draft, writing—review and editing; H.J.K.-K.: conceptualization, data curation, formal analysis, investigation, methodology, software, visualization, writing—original draft, writing—review and editing.

Both authors gave final approval for publication and agreed to be held accountable for the work performed therein.

Conflict of interest declaration. We declare we have no competing interests.

Funding. Numerical computations were partly performed using the Viking cluster, a high performance compute facility provided by the University of York. We are grateful for computational support from the University of York IT Services and Research IT team. The work of H.J.K.-K. is supported by an EPSRC Studentship.

Acknowledgements. We thank Reinhard Werner, who posed the question of whether multiple backflow was possible following talks by H.J.K.-K. and C.J.F. at the workshop *Quantum Advantages in Mechanical Systems*, IQOQI, Vienna, September 2023. We also thank Lin Htoo Zaw for useful conversations regarding the relation with Tsirelson protocols, and Simon Eveson for comments on parts of the manuscript.

References

1. Allcock G. 1969 The time of arrival in quantum mechanics III. The measurement ensemble. *Ann. Phys.* **53**, 311–348. (doi:10.1016/0003-4916(69)90253-X)
2. Bracken AJ, Melloy GF. 1994 Probability backflow and a new dimensionless quantum number. *J. Phys. A* **27**, 2197–2211. (doi:10.1088/0305-4470/27/6/040)
3. Eveson SP, Fewster CJ, Verch R. 2005 Quantum inequalities in quantum mechanics. *Ann. Henri Poincaré* **6**, 1–30. (doi:10.1007/s00023-005-0197-9)
4. Penz M, Grübl G, Kreidl S, Wagner P. 2006 A new approach to quantum backflow. *J. Phys. A* **39**, 423–433. (doi:10.1088/0305-4470/39/2/012)
5. Trillo D, Le TP, Navascués M. 2023 Quantum advantages for transportation tasks - projectiles, rockets and quantum backflow. *npj Quantum Inf.* **9**, 69. (doi:10.1038/s41534-023-00739-z)
6. Goussev A. 2021 Quantum backflow in a ring. *Phys. Rev. A* **103**, 022217. (doi:10.1103/PhysRevA.103.022217)
7. Di Bari L, Paccoia VD, Panella O, Roy P. 2023 Quantum backflow for a massless Dirac fermion on a ring. *Phys. Lett. A* **474**, 128831. (doi:10.1016/j.physleta.2023.128831)
8. Palmero M, Torrontegui E, Muga JG, Modugno M. 2013 Detecting quantum backflow by the density of a Bose-Einstein condensate. *Phys. Rev. A* **87**, 053618. (doi:10.1103/PhysRevA.87.053618)
9. Bracken AJ. 2021 Probability flow for a free particle: new quantum effects. *Phys. Scr.* **96**, 045201. (doi:10.1088/1402-4896/abdd54)
10. Barbier M, Goussev A, Srivastava SCL. 2023 Unbounded quantum backflow in two dimensions. *Phys. Rev. A* **107**, 032204. (doi:10.1103/PhysRevA.107.032204)
11. Ashfaque J, Lynch J, Strange P. 2019 Relativistic quantum backflow. *Phys. Scr.* **94**, 125107. (doi:10.1088/1402-4896/ab265c)
12. Berry MV. 2010 Quantum backflow, negative kinetic energy, and optical retro-propagation. *J. Phys. A* **43**, 415302. (doi:10.1088/1751-8113/43/41/415302)
13. Biswas D, Ghosh S. 2021 Quantum backflow across a black hole horizon in a toy model approach. *Phys. Rev. D* **104**, 104061. (doi:10.1103/PhysRevD.104.104061)
14. Bostelmann H, Cadamuro D, Lechner G. 2017 Quantum backflow and scattering. *Phys. Rev. A* **96**, 012112, 11. (doi:10.1103/PhysRevA.96.012112)
15. Yearsley JM, Halliwell JJ. 2013 An introduction to the quantum backflow effect. *J. Phys: Conf. Ser.* **442**, 012055. (doi:10.1088/1742-6596/442/1/012055)
16. Grübl G, Kreidl S, Penz M, Ruggenthaler M. 2006 Arrival time and backflow effect. In *Quantum mechanics*, AIP Conf. Proc., vol. 844, pp. 177–191. Amer. Inst. Phys., Melville, NY.
17. The FLINT team. 2022 FLINT: fast library for number theory. Version 2.9.0, https://flintlib.org.
18. Johansson F. 2019 Computing hypergeometric functions rigorously. *ACM Trans. Math. Softw.* **45**, 30, 26. (doi:10.1145/3328732)
19. Halliwell JJ, Gillman E, Lennon O, Patel M, Ramirez I. 2013 Quantum backflow states from eigenstates of the regularized current operator. *J. Phys. A* **46**, 475303, 12. (doi:10.1088/1751-8113/46/47/475303)
20. Dollard JD. 1969 Scattering into cones I: Potential scattering. *Commun. Math. Phys.* **12**, 193–203. (doi:10.1007/BF01661573)
21. Davies EB. 2007 *Linear operators and their spectra*, vol. 106. Cambridge Studies in Advanced Mathematics. Cambridge, UK: Cambridge University Press.
22. Rudin W. 1987 *Real and complex analysis*, 3rd edn. New York, NY: McGraw-Hill Book Co.
23. Kuratowski K. 1966 *Topology*, vol. I. Warsaw new edn. New York, NY: Academic Press, Państwowe Wydawnictwo Naukowe [Polish Scientific Publishers]. Translated from the French by J. Jaworowski.
24. Beer G. 1993 *Topologies on closed and closed convex sets*, vol. 268. Mathematics and its Applications. Dordrecht: Kluwer Academic Publishers Group.
25. Kato T. 1995 *Perturbation theory for linear operators*. Reprint of the 1980 edn. Classics in Mathematics. Berlin, Germany: Springer-Verlag.
26. Reed M, Simon B. 1978 *Methods of modern mathematical physics. IV. Analysis of operators*. New York, NY: Academic Press [Harcourt Brace Jovanovich, Publishers].
27. Reed M, Simon B. 1980 *Methods of modern mathematical physics. I*, 2nd edn. Functional analysis. New York, NY: Academic Press, Inc. [Harcourt Brace Jovanovich, Publishers].

28. Szegő G. 1975 *Orthogonal polynomials*, vol. XXIII, 4th edn. American Mathematical Society Colloquium Publications. Providence, RI: American Mathematical Society.
29. Fewster CJ, Kirk-Karakaya HJ. 2025 Code, datasets and animations for the paper "Repeated Quantum Backflow and Overflow", CJ Fewster and HJ Kirk-Karakaya. (doi:10.15124/6c9ec85a-7f6d-4b62-ad61-43d6f733903f)
30. Birman MS, Solomjak MZ. 1987 *Spectral theory of selfadjoint operators in Hilbert space*. Mathematics and its Applications (Soviet Series). Dordrecht: D. Reidel Publishing Co. Translated from the 1980 Russian original by S. Khrushchëv and V. Peller.
31. Matos AC. 1990 Acceleration methods based on convergence tests. *Numer. Math.* **58**, 329–340. (doi:10.1007/BF01385628)
32. Zaw LH, Scarani V. 2024 All three-angle variants of Tsirelson's precession protocol, and improved bounds for wedge integrals of Wigner functions. (http://arxiv.org/abs/2411.03132)
33. Tsirelson B. 2006 How often is the coordinate of a harmonic oscillator positive? (http://arxiv.org/abs/quant-ph/0611147)
34. Zaw LH. 2025 Precession protocols: certifying nonclassicality with oscillations and rotations. PhD thesis, National University of Singapore.
35. Fewster CJ, Kirk-Karakaya HJ. 2025 Repeated quantum backflow and overflow. Figshare. (doi:10.6084/m9.figshare.c.8174360)